Lunar Mass Driver Implementation

a project presented to
The Faculty of the Department of Aerospace Engineering
San Jose State University

in partial fulfillment of the requirements for the degree
Master of Science in Aerospace Engineering

by

Ethan J. Miller

May 2023

approved by

Dr. Periklis Papadopoulos
Faculty Advisor

ABSTRACT
Lunar Mass Driver Implementation

Ethan J. Miller

After nearly five decades, mankind is planning to return to the Moon with the intent of setting up a colony. This colony could accomplish several important scientific studies and breakthroughs, but a lunar colony also presents the potential to harvest the Moon's natural resources. This paper expands on the work performed by a team of NASA scientists led by Dr. Gerard O'Neill who designed a lunar mass driver capable of transporting harvested lunar resources back to Earth. Specifically, this paper focuses on the design of the communications, thermal, and power subsystems which would make a mass driver functional. This paper also examines potential trajectories for the mass driver utilizing the restricted circular planar three-body problem approach. The design and trajectory analysis were performed utilizing MATLAB and utilizing techniques outlined in Space Mission Analysis and Design. The result are subsystems which enable a functioning lunar mass driver capable of transferring 100,000 metric tons of lunar material from the Moon to low Earth orbit for a mission life of 20 years.

Acknowledgements

Table of Contents

List of Tables

List of Figures

Symbols

Symbol	Definition	Units (SI)
m	Mass	kg
f	Frequency	Hz
v	Velocity	m/s
a	Acceleration	m/s^2
$\dot{m}$	Mass Throughput Rate	kg/s
D	Caliber/Diameter	m
S	Section/Path Length	m
M	System Mass	kg
P	Power	W
W	Width	m
r	Radius	m
ℓ	Length	m
V	Volume	m^3
i	Current	A
H	Inductance	H
N	Number	------------------
R	Data Rate	Bps
e	Pointing Error	degrees°
L	Loss	dB
T	Temperature	K
E_b/N_o	Signal to Noise Ratio	dB
θ	Beam Width	degrees°
B	Gain	dB
A	Area	m^2
Q	Heat	W
q	Heat Flux	W/m^2
t	Time	hrs
X	Path Efficiency	------------------
C	Capacity	W*hr
DOD	Depth of Discharge	%
n	Battery Line Efficiency	------------------
G	Gravitational Constant	m^3/s^2kg
x	X-Distance from Barycenter	km
$\ddot{x}$	X-Acceleration	km/s^2
$\ddot{y}$	Y-Acceleration	km/s^2
$\ddot{z}$	Z-Acceleration	km/s^2
$\dot{x}$	X-Velocity	km/s
$\dot{y}$	Y-Velocity	km/s
$\dot{z}$	Z-Velocity	km/s
z	Z-Distance from Barycenter	km
y	Y-Distance from Barycenter	km

Symbol	Definition	Units (SI)
Greek Symbols		
ρ	Density	kg/m^3
η	Efficiency	-----------------
σ	Boltzmann Constant	W/m^{2}K^4
ε	Emissivity	------------------
ω	Angular Velocity	Rad/s
τ	Orbital Period	Seconds
Subscripts		
()$_1$	Payload Mass	-----------------
()$_p$	Payload	-----------------
()$_R$	Payload Rate	-----------------
()$_e$	Exhaust	-----------------
()$_B$	Bucket	-----------------
()$_{BL}$	Loaded Bucket	-----------------
()$_a$	Accelerating	-----------------
()$_d$	Decelerating	-----------------
()$_{tot}$	Total	-----------------
()$_{SCR}$	SCR	-----------------
()$_W$	Winding	-----------------
()$_F$	Feeder	-----------------
()$_{kin}$	Kinetic	-----------------
()$_{el}$	Electrical	-----------------
()$_{st}$	Structural	-----------------
()$_p$	Phase	-----------------
()$_{BC}$	Bucket Coil	-----------------
()$_{super}$	Superconductor	-----------------
()$_S$	Single-turn	-----------------
()$_r$	Receiver	-----------------
()$_t$	Transmitter	-----------------
()$_l$	Transmitter Line	-----------------
()$_{ab}$	Absorptivity	-----------------
()$_s$	System Noise	-----------------
()$_{tp}$	Transmitter Peak	-----------------
()$_{rp}$	Receiver Peak	-----------------
()$_{int}$	Internal	-----------------
()$_{ext}$	External	-----------------
()$_{ec}$	Eclipse	-----------------
()$_{sa}$	Solar Array	-----------------
()$_{dl}$	Daylight	-----------------
()$_o$	Original	-----------------
()$_{BOL}$	Beginning of Life	-----------------
()$_{dg}$	Degradation	-----------------
()$_{EOL}$	End of Life	-----------------

Symbol	Definition	Units (SI)
()$_b$	Battery	-----------------
()$_{ea}$	Earth	-----------------
()$_m$	Moon	-----------------
()$_{Payload}$	Payload	-----------------
Acronyms		
NASA	National Aeronautics and Space Administration	-----------------
SCR's	Silicon-Controlled Rectifiers	-----------------
SLS	Space Launch System	-----------------
SSME	Space Shuttle Main Engine	-----------------
LEO	Low Earth Orbit	-----------------
SMAD	Space Mission Analysis and Design	-----------------
BER	Bit Error Rate	-----------------
TCS	Thermal Control Subsystem	-----------------
IR	Infrared	-----------------
EPS	Electrical Power Subsystem	-----------------
DET	Direct-Energy Transfer	-----------------
GEO	Geostationary Earth Orbit	-----------------
ISS	International Space Station	-----------------

1. Introduction

1.1 Motivation

In 1969 humanity took its first steps on the Moon. Since then, only a handful of people have stepped foot on the Moon, and none since the end of the Apollo missions. Over the last decade, there has been a renewed interest in space exploration, and specifically, a renewed interest in returning to the Moon. As a part of this renewed interest, NASA and commercial interests are examining ways to set up permanent infrastructure on the Moon [1].

There are several potential reasons to set up a permanent infrastructure on the Moon including:

- Helium-3, methane, ice, and platinum mining [2]
- Solar energy collection [2]
- Launch pad for deep-space exploration [3]
- Interference-free radio-telescopes and antennae [3]
- Trial-run for a potential Mars colony [1]

Each of these potential reasons for setting up a lunar colony has advantages and disadvantages, but the most commercially viable reason is mining.

Helium-3 is not readily abundant on Earth, and what little there is on Earth, is concentrated in a couple of areas under the control of a handful of governments. Currently Helium-3 is being examined as a potential material for nuclear fusion, but the low supply of Helium-3 makes it less than ideal. The Moon is constantly bombarded by solar wind which has been depositing trace amounts of Helium-3 across the surface of the Moon for billions of years. This makes the Moon a potentially abundant source of Helium-3 [1].

Methane and ice mining could be useful for any lunar colony. Methane is useful as a propellant and a source of heat, and more recent experiments indicate it could be useful for the production of oxygen. Ice provides a source of water independent from Earth, enabling a lunar colony to be self-sufficient. If in the future other colonies are built on Mars or in the asteroid belts, the Moon's methane and ice could have another role to play.

It is much easier to travel from the Moon to another location in the solar system than it is to travel from Earth. Specifically, a rocket launching from Earth requires nearly five times the amount of delta-v that would be required if that same rocket launched from the Moon instead. This means the Moon could function as a more efficient source of fuel and water to colonies scattered across the solar system if a reliable method of transport could be developed [1].

One such method of transport is a mass driver. A mass driver utilizes magnetic fields to propel a payload into space. The advantage of a mass driver over a traditional rocket is that a mass driver does not rely on propellant to launch a payload into orbit. Instead, solar panels can be used to gather the electricity required to power the magnetic fields used in the mass driver to accelerate the payload.

In 1977, Dr. Gerard K. O'Neill led a team of scientists at NASA who explored the possibility of a mass driver for use transporting small payloads from the Moon into low Earth orbit [4]. Due to political and economic pressures, the work done by Dr. O'Neill stalled and only a small preliminary test model was built. However, now there is renewed government and commercial interest in a permanent colony on the Moon, meaning there is a use for this previously shelved concept.

The initial work performed by Dr. O'Neill's team focused on the design of the mass driver, leaving the design of the infrastructure supporting the mass driver as a future project. Now the many advancements in technology since the 1970's can be used to design the systems and infrastructure required to make a lunar mass driver functional.

1.2 Literature Review

1.2.1 Mass Driver Design

Dr. O'Neill and his team began their research into a mass driver lunar launch system in 1977 for NASA. Rather than design a specific mass driver, the team created a concept for a potential mass driver system and then derived the equations necessary to customize the design. The concept created utilized small buckets of superconducting coils which would carry payloads [4].

The buckets would be accelerated using magnetic fields until the desired velocity was achieved, at which point the payload would be released. The buckets would then be decelerated on a parallel track and refilled with additional payload. The idea was to create a system like a conveyor belt which could continuously launch payloads toward low Earth orbit.

O'Neill's team derived a series of equations which would take five design variables as inputs, and generate the total system mass, power required, and size as outputs. Specifically, the required inputs were:

- Mass of the payload, m_1 (kg)
- Density of the payload, ρ_P (kg/m^3)
- Launch rate of payload, f_R (Hz)
- Launch velocity, v_e (m/s)
- Acceleration imparted on the bucket, a (m/s^2)

Using these five parameters, all the design elements of the mass driver could be derived.

While O'Neill and the team derived the equations required to design a mass driver, they pointed out certain key areas that could be improved including:

- Lighter radiators
- Silicon-controlled rectifiers (SCR's) with higher temperature ratings
- Higher energy density capacitors

Having lighter radiators would make the overall structure lighter and cheaper to build, while also making the structure potentially easier to transport to the Moon. SCR's with a higher temperature

rating would mean the system temperature could be increased to 440 K, which is the optimal system temperature to minimize powerplant and radiator mass. Finally, higher energy density and specific mass capacitors with a service life of approximately 10^{10} discharge cycles would be required to make the mass driver operational.

1.2.2 Capacitor Technology

Energy storage is a critical element of any mass driver, as the magnetic fields created to propel a payload are sizable. To generate the required magnetic field strength, a large amount of energy must be discharged in a very short time span at a very high voltage [4]. The ideal form of energy storage for this specific requirement is a capacitor. Capacitors, unlike batteries, can discharge nearly all the stored energy within fractions of a second, making capacitors ideal in this scenario.

Capacitor technology has existed for a long time as a method for storing and then quickly discharging electricity. Originally, a capacitor consisted of two flat metal plates separated from each other by a thin dielectric film [5]. While this was the case, batteries proved to be the preferred method of energy storage as they could hold more electricity than these original capacitors.

As technology continued to advance, greater energy density storage became necessary, and battery energy density advancements began to stall. At the same time, advancements in manufacturing techniques revolutionized capacitors. Rather than using two flat plates, two very thin metal sheets were rolled up and stacked on each other, expanding the effective surface area of the capacitor, increasing the energy storage capacity [5].

The new limit for capacitors was now dictated by how tightly the metal sheets could be rolled [5]. These new "ultra-capacitors" provide a viable energy storage and discharge solution for a lunar mass driver. In their initial design, O'Neill's team noted that capacitors were not sufficiently energy dense enough for a mass driver. This was because the overall length of the mass driver, and the length of each sector of the mass driver, was partially determined by the specific mass (J/kg) of the capacitors.

At the time, capacitors with the required energy density and life cycle had a specific mass less than one tenth of the necessary specific mass. This would mean the mass driver sector length would need to be increased and correspondingly, an increased discharge rate, further reducing the effectiveness of the suboptimal capacitors [4].

New ultra-capacitors provide a solution to this issue. Ultra-capacitors are now available with more than sufficiently high specific mass. However, one major concern is that the life cycle of these ultra-capacitors is not as high as desired by O'Neill's team [4, 5]. Additionally, ultra-capacitors have not been tested in a lunar environment, which may have a negative impact on life cycle. This less-than-ideal life cycle can be partially accounted for by reducing the discharge rate. It is possible that by taking advantage of the increased specific mass and energy density of ultra-capacitors, the payload size could be increased to retain a similar mass throughput as the one O'Neill's team designed for.

1.2.3 Thermal Control Technology

Thermal control is an integral part of a lunar mass driver. The temperature of the electrical components must be kept low enough to prevent hardware failure. When O'Neill's team was designing the lunar mass driver they identified radiators as being the method that the temperature of the SCR's and superconductors would be regulated.

Radiators are one of the few ways to disperse heat in space, but over the years there are several additional methods which have been experimented with and refined. Specifically, heat pipes enable heat to be transferred through conduction, which is a more volume-efficient method of heat transfer than radiation [6]. Heat pipes provide an interesting alternative or complement to radiators which could reduce the overall volume, potentially reducing the launch cost of a lunar mass driver.

1.2.4 Lunar Topography

Over the years, humanity has had many theories regarding the make-up and topography of the Moon. When the first telescopes gave astronomers a much closer glimpse of the Moon, it was believed that the Moon had seas and continents of its own, the maria and highlands respectively [2]. Now, we know that the "seas" seen by early astronomers were regions full of basalt from volcanic activity hundreds of millions of years ago [2, 7].

In addition to the maria and highlands, the Moon has two poles which have specific factors which make them potentially ideal locations for a lunar mass driver. Each pole has locations where a solar farm could be placed to nearly always be in direct sunlight [1]. The advantage of this is that there would always be electricity being generated. For the purposes of a lunar mass driver, the capacitors would always be able to be charged.

The other factor which makes the poles an ideal location for a lunar mass driver is the likely presence of ice within polar traps [2]. Being near the presence of frozen water would mean that a lunar colony associated with the lunar mass driver would have a nearby source of water. Additionally, if the Moon is used a staging point for other colonies amongst the asteroid belt or Mars, proximity to ice enables ice to be transported to those other colonies by the mass driver.

1.2.5 Transport to Moon

When NASA tasked Dr. O'Neill and his team to develop a lunar mass driver, a central concern was how to get the mass driver to the Moon. At the time, the Space Shuttle was under development and no other spacecraft was capable of transporting a mass driver weighing between 50 and 100 metric tons [8]. As a result, the mass driver was designed to be broken down into hundreds of smaller cells which would be put together on the Moon. This would enable the entire structure to be transported to the Moon aboard 12-19 Space Shuttle launches given the expected payload capacity of the Space Shuttle at the time [4, 9]. It was determined that that many launches were prohibitively expensive at the time, and when the launch and development cost of the Space Shuttle increased, it further cemented the mass driver as uneconomical [10].

The last decade, however, has seen a change in spacecraft design. Specifically, the movement towards commercialization of space travel and exploration has led companies to begin designing rockets that have the capability to transport as much as 130 metric tons of payload into low Earth orbit [11]. Currently SpaceX's Falcon Heavy rocket is expected to be able to lift nearly 64 metric tons into low Earth orbit. From there, SpaceX intends to launch a second Falcon Heavy to refuel the first rocket, allowing it to take its 64 metric ton payload to the Moon or to Mars [12].

Alongside SpaceX, NASA has also been developing a heavy lift rocket capable of transporting up to 130 metric tons of payload to low Earth orbit, or up to 46 metric tons of payload directly to the Moon. This Space Launch System (SLS) utilizes the Space Shuttle main engine (SSME) and has several different payload volume configurations [11]. Both the SLS and Falcon Heavy rockets present the possibility of transporting all the components for a lunar mass driver to the Moon with only a couple of launches. This is a huge improvement when compared to the 12 to 19 launches that would have been required of the Space Shuttle.

Additionally, these new classes of rocket enable the infrastructure to be built which would make a lunar mass driver useful. Specifically, these rockets can transport the habitats required to set up a lunar colony or lunar mining outpost, without which a lunar mass driver would have no use [1].

1.3   Project Proposal

Now that technology has advanced to the point where the few missing elements of the mass driver proposed by Dr. O'Neill and his team exist, the systems supporting a lunar mass driver can be designed. The objective of this project is to utilize the mass driver designed by Dr. O'Neill's team as a functional black box. The inputs will be determined by requirements and will serve as the design variables required to utilize the mass driver design equations derived by Dr. O'Neill's team [4]. The outputs from the mass driver design equations will be utilized to design the systems required to support the mass driver including:

- Power system
- Thermal control system
- Communication system

Once the systems have been designed, a trajectory analysis will be performed to ensure the payload reaches low Earth orbit.

1.4   Methodology

The specific steps that will be taken for this project are:

- Research background information regarding the Moon and mass driver design to determine ideal mass driver location.
- Determine payload requirements for mass driver, providing mass driver inputs.
- Utilizing mass driver inputs, calculate the outputs.

- With the outputs, design the support systems for mass driver and perform trajectory analysis.
- Refine systems and trajectory as necessary.
- Examine potential consequences of lunar mass driver.

2. System Requirements

2.1   Mass Driver Requirements

The requirements which define the mass driver, and subsequently the subsystems that support the mass driver are:

- The mass driver shall have a mass throughput of at least 100,000 metric tons per year.
- The payload from the mass driver shall be launched on a trajectory that ends in a stable low Earth orbit.
- The mass driver shall operate for a mission life of 20 years.

For the purposes of this project, it will be assumed that the mass driver is capable of meeting these requirements. This is to allow the focus of this project to be on the design of the subsystems which will enable the mass driver to meet these requirements.

2.2   Power Subsystem Requirements

The requirements which define the power subsystem are:

- The power subsystem shall provide at least 8.7 MW to the mass driver while the mass driver is operational.
- The power subsystem shall provide enough power to operate the active component of the thermal control subsystem.
- The power subsystem shall provide enough power to operate the communications subsystem.

The specific numbers associated with each of these requirements have been (or will be) determined during the design process. Mathematical analysis will be used to verify that the power subsystem meets each requirement.

2.3   Thermal Control Subsystem Requirements

The requirements which define the thermal control subsystem are:

- The thermal control subsystem shall maintain an operational temperature less than 400 K across the entire mass driver.
- The thermal control subsystem shall maintain an operational temperature between 233 K and 343 K for the control electronics.

The operational temperatures required are based on the operational temperatures outlined by O'Neill's team in their initial mass driver design [4]. Mathematical analysis will be used to verify that the thermal control subsystem meets each requirement.

2.4   Communications Subsystem Requirements

The requirements which define the communications subsystem are:

- The communications subsystem shall enable at least 25 kbps data transfer from the mass driver to an Earth ground station.
- The communications subsystem shall enable at least 1 kbps data transfer from an Earth ground station to the mass driver.
- The communications subsystem shall enable at least 25 kbps data transfer between the mass driver and a lunar colony.

These data transfer values provide a communications baseline and were an agreed upon requirement between the author and project advisor. Mathematical analysis will be used to verify that the communications subsystem meets each requirement.

3. Mass Driver Parameters

3.1 Mass Throughput Rate

The first two design variables for a lunar mass driver, according to O'Neill's team [4], are the mass and launch rate of the payload. Together, these variables result in the mass throughput rate of the mass driver. For this project, a desired mass throughput rate for the mass driver shall be selected as 100,000 metric tons per year.

In section 1.2.4, the lunar poles were identified as ideal locations for a lunar colony and by extension a lunar mass driver. With the solar panels nearly always in sunlight at the lunar pole, the mass driver is assumed to have an 80% uptime. This allows for emergency repair downtime, and accounts for times the solar panels aren't in sunlight.

With 80% uptime, and a requirement of 100,000 metric tons per year, the required mass throughput rate in kg/s can be derived:

$$\dot{m} = (100,000 \ t/yr) * 0.8 * \left(\frac{1 \ yr}{31,536,000 \ s}\right) * \left(\frac{1,000 \ kg}{1 \ t}\right) = 2.54 \ kg/s \qquad (3.1)$$

Rather than launch payload every second, which might present logistical problems with regard to loading payload, payload will be launched every ten seconds, a launch frequency of 0.1 Hz. This results in each launch having a mass of 25.4 kg. Lunar regolith has a density of approximately 1.5 g/cm³ [13], or 1,500 kg/m³. Using the payload mass and payload density, the caliber of the mass driver can be determined using O'Neill's team's equations [4]:

$$D = \left(\frac{m_1}{(6.538 * 10^{-2})\rho_P}\right)^{\frac{1}{3}} = \left(\frac{25.4 \ kg}{(0.06538)(1500 \ kg/m^3)}\right)^{\frac{1}{3}} = 0.637 \ m \qquad (3.2)$$

The caliber is defined as the mean diameter of the drive coils [4] and is a key design parameter for a mass driver.

3.2 Launch Velocity

The launch velocity is the velocity of the payload once it has exited the mass driver. Since the intent is to launch the payload to low Earth orbit (LEO), the launch velocity must be at least equal to the lunar escape velocity. While the lunar escape velocity is 2.38 km/s, 2.4 km/s will be used as this gives a small margin for error and simplifies the computations.

3.3 Mass Driver Acceleration

The acceleration of the mass driver is the acceleration imparted upon the payload and the payload bucket by the magnetic drive force of the mass driver. The higher the acceleration of the mass driver, the shorter the overall length of the mass driver. Additionally, higher accelerations

have increased power and thermal requirements. This trade-off between mass driver length and power and thermal requirements should be investigated and analyzed in a future project to determine the optimal acceleration for a lunar mass driver.

For this design, an acceleration of 1,000 Earth gravities, or 9,800 m/s² shall be used. This is the number used by O'Neill's team in their calculations and provides a solid benchmark for future optimization [4].

3.4 Mass Driver Derived Parameters

Utilizing the parameters determined earlier in this section, the remaining design parameters can be calculated using O'Neill's team's equations. The goal of these equations is to eventually determine the overall system mass, power required, and thermal load, as these values will define the design of the subsystems supporting the mass driver.

A table summarizing the design parameters can be found at the end of this section, while the remaining design parameters will be calculated now. Several of the parameters in the equations below are derived in Appendix A.

3.4.1 Mass Driver Length Derivation

Length of accelerating section:

$$S_a = \frac{v_e^2}{2a} = \frac{(2400 \ m/s)^2}{2*(9800 \ m/s^2)} = 293 \ m \tag{3.3}$$

Length of decelerating section:

$$S_d = \left(\frac{m_B}{m_{BL}}\right)\left(\frac{v_e^2}{2a}\right) = (0.69)(293 \ m) = 202 \ m \tag{3.4}$$

Total length of mass driver:

$$S_{tot} = \ S_a + S_d = (293 \ m) + (202 \ m) = 495 \ m \tag{3.5}$$

3.4.2 Mass Driver System Mass Derivation

Total SCR mass:

$$M_{SCR} = (1.656*10^{-10})v_e^3 a m_1^{\frac{1}{3}} = (1.656*10^{-10})\left(2400\frac{m}{s}\right)^3\left(9800\frac{m}{s^2}\right)(25.4 \ kg)^{\frac{1}{3}} \tag{3.6}$$
$$= 65{,}950 \ kg$$

Total winding mass:

$$M_W = (0.142)v_e^{\frac{3}{2}}m_1^{\frac{1}{2}}f_R^{\frac{1}{2}} = (0.142)\left(2400\,\frac{m}{s}\right)^{\frac{3}{2}}(25.4\,kg)^{\frac{1}{2}}(0.1\,Hz)^{\frac{1}{2}} = 26{,}600\,kg \qquad (3.7)$$

Total feeder mass:

$$\begin{aligned}
M_F &= (7.973 * 10^{-4})v_e^{\frac{5}{3}}a^{\frac{1}{3}}m_1^{\frac{5}{9}}f_R^{\frac{1}{3}} \\
&= (7.973 * 10^{-4})\left(2400\,\frac{m}{s}\right)^{\frac{5}{3}}\left(9800\,\frac{m}{s^2}\right)^{\frac{1}{3}}(25.4\,kg)^{\frac{5}{9}}(0.1)^{\frac{1}{3}} \\
&= 20{,}550\,kg
\end{aligned} \qquad (3.8)$$

Kinetic power mass:

$$\begin{aligned}
M_{kin} &= 0.5f_R m_1 m_p v_e^2 = (0.5)(0.1\,Hz)(25.4\,kg)\left(0.014\,\frac{kg}{W}\right)\left(2400\,\frac{m}{s}\right)^2 \\
&= 102{,}400\,kg
\end{aligned} \qquad (3.9)$$

Total electrical mass:

$$\begin{aligned}
M_{el} &= M_S + 2M_W + 3M_F + M_{kin} \\
&= (65950\,kg) + 2(26600\,kg) + 3(20550\,kg) + (102400\,kg) \\
&= 283{,}200\,kg
\end{aligned} \qquad (3.10)$$

Total structural mass:

$$M_{st} = 0.5M_{el} = 0.5(283200\,kg) = 141{,}600\,kg \qquad (3.11)$$

Total mass of mass driver system:

$$M_{tot} = M_{el} + M_{st} = (283200\,kg) + (141600\,kg) = 424{,}800\,kg \qquad (3.12)$$

3.4.3 Mass Driver Power Requirement Derivation

Mass driver power requirement:

$$\begin{aligned}
P_{tot} &= M_{kin}\frac{1}{m_p} + (M_W + M_F)\frac{1}{m_p + m_R} = \frac{102400\,kg}{0.014\,\frac{kg}{W}} + \frac{26600\,kg + 20550\,kg}{0.014\,\frac{kg}{W} + 0.02\,\frac{kg}{W}} \\
&= 8.7 * 10^6 W
\end{aligned} \qquad (3.13)$$

Waste power:

$$P_W = \frac{(M_W + M_F)}{m_p + m_R} = \frac{(26600 \; kg + 20550 kg)}{0.014 \frac{kg}{W} + 0.02 \; kg/W} = 1.39 * 10^6 \; W \tag{3.14}$$

Mass driver efficiency:

$$\eta = \frac{P_{tot} - P_W}{P_{tot}} = \frac{8.7 * 10^6 \; W - 1.39 * 10^6 \; W}{8.7 * 10^6 \; W} = 0.84 = 84\% \tag{3.15}$$

Table 3.1- Mass driver dependent system parameters

Dependent Parameter	Calculated Value
SCR Mass	$6.60*10^4$ kg
Winding Mass	$2.66*10^4$ kg
Feeder Mass	$2.06*10^4$ kg
Kinetic Power Mass	$1.02*10^5$ kg
Total Electric Mass	$2.83*10^5$ kg
Total Mass	$4.25*10^5$ kg
Total Length	$4.95*10^2$ m
Waste Power	$1.39*10^6$ W
Total Power	$8.7*10^6$ W
Efficiency	84%

4. Communications Subsystem

4.1   Requirements

The requirements for the communications subsystem outlined in chapter 2 are:

- The communications subsystem shall enable at least 25 kbps data transfer from the mass driver to an Earth ground station.
- The communications subsystem shall enable at least 1 kbps data transfer from an Earth ground station to the mass driver.
- The communications subsystem shall enable at least 25 kbps data transfer between the mass driver and a lunar colony.
- The communications subsystem shall have a link margin of at least 10 dB to account for poor weather conditions during data transfer.

The data that will be transmitted from the mass driver to the lunar colony and Earth ground station includes:

- Temperature measurements from superconducting segments.
- Exit velocity at each payload launch.
- Launch trajectory of each payload.
- System warnings or errors.

The data that the mass driver communications subsystem will receive from the Earth ground station and lunar colony includes:

- Launch frequency.
- System commands.

The requirements for the communications subsystem will allow the desired data to be transmitted and received by the lunar mass driver. The necessary power will be determined in the next section by analyzing the link budget for the subsystem, as well as outlining the data flow.

4.2   Historical Communications Architecture

Traditionally, spacecraft communications systems have been comprised of a series of specially manufactured analog circuits designed to survive the harsh environment of space. Due to analog circuits not being particularly adaptable, a series of analog circuits designed for specific tasks was required, resulting in a "communications stack" [14]. This communications stack, while fully space tested and ready, is technologically outdated when compared to modern terrestrial communication standards.

More recently, spacecraft have begun to use field programmable gate arrays (FPGA) as a replacement for the analog communications stack. The advantage of FPGAs is that FPGAs are highly adaptable and flexible and can be programmed to accomplish each of the operations previously accomplished by each component of the communications stack. An FPGA can be

manufactured to withstand the harsh environment of space and has the advantage of not requiring a specialized factory for production. An FPGA cannot replace an antenna, but it can replace the other elements in a communications stack, performing all the replaced functions faster and in a smaller package [14].

4.3 Architecture

To meet the communications subsystem requirements, the architecture that will be used is shown below in Figure 4.1. Each of the elements aside from the antenna will be a subfunction on a FPGA rather than an individual analog circuit. For the transmission of information from the mass driver, data will be sent to an encoder and then sent to a transmitter where it will pass through a low-pass filter and a diplexer before being beamed to either an Earth ground station or a lunar colony. To receive data or commands from an Earth ground station or a lunar colony, the diplexer will convert the transmitting antenna to a receiving antenna before passing the received data through a decoder and sending the information to the mass driver.
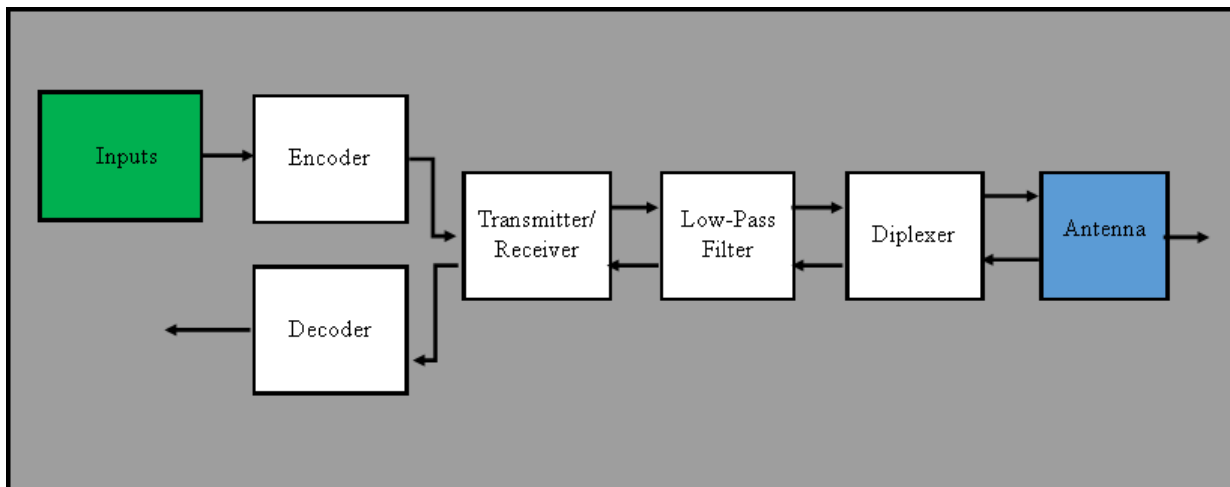
Figure 4.1- Block diagram of communications architecture

Additional elements such as a specific modulation and coding scheme and antenna size will be determined after a mathematical analysis is performed on the effect of these elements on required subsystem power. For this design, a desired link margin and bit rate for both uplink and downlink were given in the requirements. These values enable the required transmitter power to be calculated. The following calculations are based on the equations outlined for link budget design in the book Spacecraft Mission Analysis and Design (SMAD) [15].

4.4 Transmitter Power Calculations

The governing equation for the design of the communications subsystem is the link equation which can be found in SMAD [15]:

$$\frac{E_b}{N_o} = \frac{P L_l B_t L_s L_a B_r}{k T_s R}$$

(4.1)

This equation provides a mathematical relationship between the transmitter power, antenna gain and size, data rate, and system losses with the signal-to-noise ratio of the subsystem. The system losses are broken down into several categories and can all be determined by analyzing historical trends, or be directly calculated. The transmitter power, antenna gain and size, and the data rate are all design variables that can either be defined or solved for. For this project, the data rate is specified in the requirements and the transmitter power is the variable that will be solved for, so the antenna size will be defined as the main input parameter.

Since the mass driver will be communicating with both an Earth ground station and a lunar colony, two separate calculations will be required. Only the calculations performed to find the required transmitter power in the Earth ground station case will be shown below, but the calculations for the lunar colony case can be found in Appendix B. Table 4.1 displays the values of the input parameters and system losses that will be utilized to calculate the required transmitter power for the Earth ground station case.

Table 4.1- Transmitted power input parameters

Parameter	Value
Link Margin	10 dB
Implementation Losses	-2 dB
Bit Error Rate (BER)	10^{-5}
Data Rate (R)	25 kbps
Receive Antenna Pointing Error (e_r)	0.2°
Receive Antenna Diameter (D_r)	5 m
Propagation Path Length (S)	3.85×10^8 m
Transmit Antenna Pointing Offset (e_t)	0.5°
Transmit Antenna Diameter (D_t)	5 m
Transmitter Line Loss (L_l)	-1 dB
Frequency (f)	2 GHz
Absorption Loss (L_{ab})	-3.4 dB
System Noise Temperature (T_s)	135 K

To calculate the transmitter power required, first the desired E_b/N_o is calculated:

$$E_b/N_o = (E_b/N_o)_{Req} - Implementation\ Loss + Link\ Margin$$
$$= 9.6\ dB - (-2\ dB) + 10\ dB = 21.6\ dB$$

(4.2)

The required E_b/N_o was obtained from SMAD [15] assuming the use of either binary phase shift keying or quadriphased phase shift keying modulation and coding scheme. This selection was made as a preliminary selection and an analysis of alternative modulation and coding schemes will be performed later in this chapter.

With the desired E_b/N_o calculated, the required transmitter power can be determined utilizing the transmitter gain, space loss, receiver gain, and system noise temperature calculated below.

Transmitter antenna gain:

$$\theta_t = \frac{21}{fD_t} = \frac{21}{(2\ GHz)(5\ m)} = 2.1° \tag{4.3}$$

$$B_{tp} = 44.3 - 10\log(\theta^2) = 44.3 - 10\log(2.1°^2) = 37.9\ dB \tag{4.4}$$

$$L_{tp} = -12\left(\frac{e}{\theta}\right)^2 = -12\left(\frac{0.5°}{2.1°}\right)^2 = -0.68\ dB \tag{4.5}$$

$$B_t = B_{tp} + L_{tp} = 37.9\ dB + (-0.68\ dB) = 37.2\ dB \tag{4.6}$$

Space loss:

$$
\begin{aligned}
L_s &= 147.55 - 20\log(S) - 20\log(f) \\
&= 147.55\ dB - 20\log(3.85 * 10^8\ m) - 20\log(2 * 10^9\ Hz) \\
&= -210\ dB
\end{aligned} \tag{4.7}
$$

Receiver antenna gain:

$$
\begin{aligned}
B_{rp} &= -159.59 + 20\log(D) + 20\log(f) + 10\log(\eta) \\
&= -159.59\ dB + 20\log(5\ m) + 20\log(2 * 10^9\ Hz) + 10\log(0.55) \\
&= 37.8\ dB
\end{aligned} \tag{4.8}
$$

$$\theta_r = \frac{21}{fD_r} = \frac{21}{(2\ GHz)(5\ m)} = 2.1° \tag{4.9}$$

$$L_{rp} = -12\left(\frac{e}{\theta}\right)^2 = -12\left(\frac{0.2°}{2.1°}\right)^2 = -0.11\ dB \tag{4.10}$$

$$B_r = B_{rp} + L_{rp} = 37.8\ dB + (-0.11\ dB) = 37.7\ dB \tag{4.11}$$

Transmitter power:

$$
\begin{aligned}
P_t &= E_b/N_o - L_l - B_t - L_s - L_{ab} - B_r - 228.6 + 10\log(T_s) + 10\log(R) = \\
&21.3\ dB - (-1\ dB) - 37.2\ dB - (-210\ dB) - (-3.4\ dB) - 37.7\ dB - 228.6\ dB + \\
&10\log(135\ K) + 10\log(25 * 10^3) = -2.52\ dB = 0.56\ W
\end{aligned} \tag{4.12}
$$

An identical process was followed to determine the transmitter power required for the mass driver to communicate with a lunar colony 10 km away from the mass driver. The specific calculation was performed in MATLAB and the code can be found in Appendix B, but the resulting required transmitter power is 4.21e[-10] W.

4.5   Communications Subsystem Analysis

Evidently, the required transmitter power for communication with both the Earth ground station and the lunar colony is nearly inconsequential when compared to the power requirement

for the mass driver. It is likely that the reason for such a small transmitter power is due to the large diameter of the antenna.

In order to determine the effect of the antenna diameter on the transmitter power the MATLAB program performing the calculations was expanded. The antenna diameter was changed from a single value to an array of values in MATLAB ranging from 0.5 m to 5 m in increments of 0.1 m. The resulting transmitter power was plotted against the antenna diameter resulting in Figure 4.2 below.
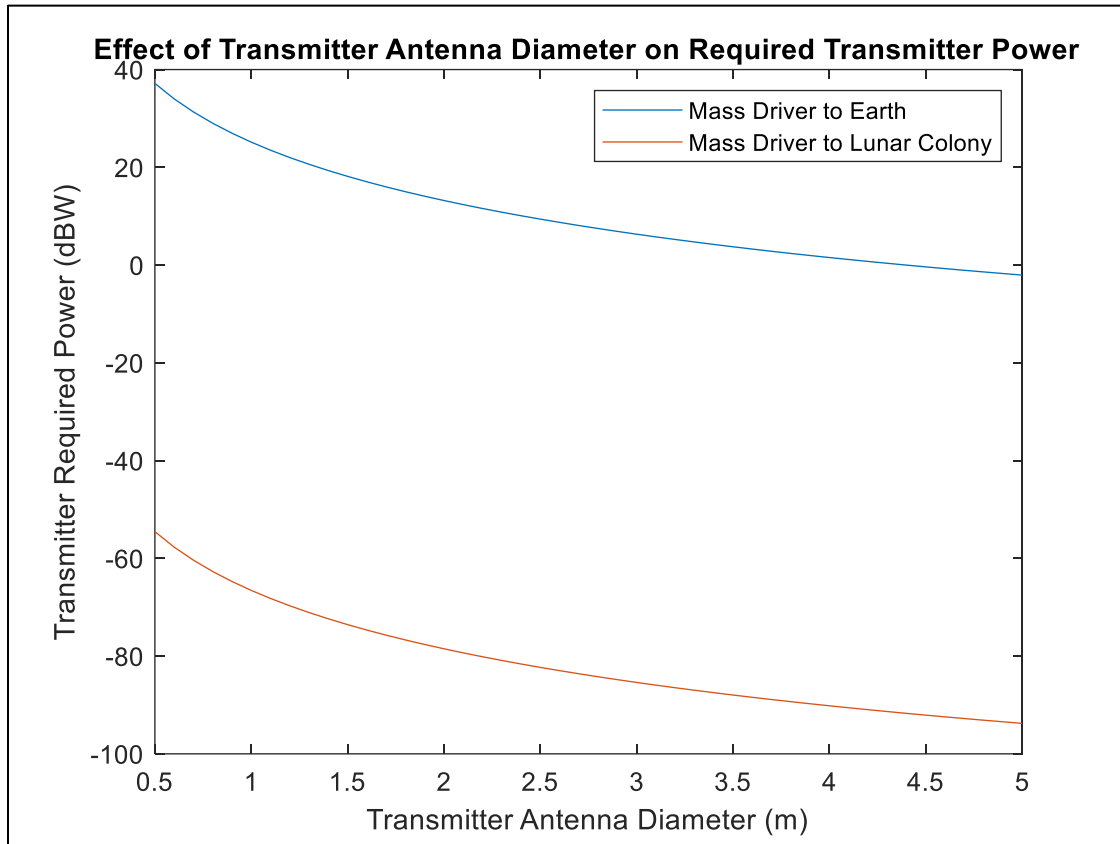
Figure 4.2- Effect of transmitter antenna diameter on required transmitter power

Figure 4.2 shows the effect of antenna diameter on the transmitter power for both the Earth ground station and the lunar colony cases. It can be seen in Figure 4.2, that as the antenna diameter increases, the required power decreases. The comparison of the curves in each figure indicates that the power required for the mass driver to communicate with the lunar colony will always be less than the power required to communicate with an Earth ground station. This makes intuitive sense and when coupled with the fact that the mass driver will only utilize a single antenna means that the power required to communicate with an Earth ground station is the system-defining variable. As such the Earth ground station case will be the primary focus of continued analysis, while the lunar colony case will be assumed to be achievable if the Earth ground station case is achievable.

Another potential variable to examine is the type of modulation and coding utilized during communication. The calculations earlier in this section assumed either a binary or quadriphased phase shift keying modulation and scheme, but SMAD [15] presents several other potential options. The main effect changing the modulation and coding scheme will have on the calculations is it will change the required E_b/N_o value. Figure 4.3 shows the effects of each modulation and coding scheme on the required transmitter power.
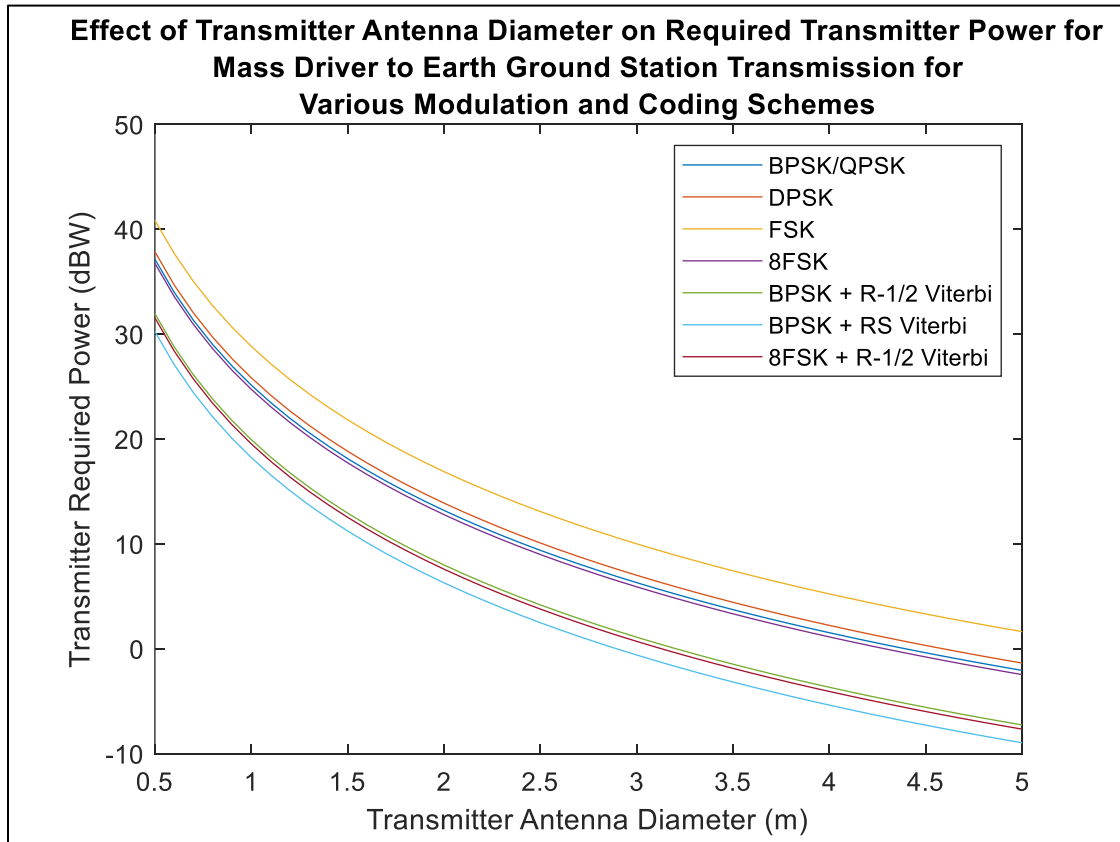
Figure 4.3- Effect of antenna diameter and modulation schemes on required transmitter power

Figure 4.3 shows that the type of modulation and coding scheme appears to have no effect on the overall trend between the antenna diameter and transmitter power. The modulation and coding scheme appears to only shift the magnitude of the trend. The most power intensive modulation and coding scheme is the frequency shift keying which makes sense as SMAD [15] indicates that this scheme has the highest required E_b/N_o. The advantage of this scheme is that it, along with other frequency shift keying schemes, is generally not susceptible to phase disturbances. However, the disadvantage is the higher required transmitter power necessary to perform this scheme.

The least power intensive scheme is the binary phase shift keying scheme with RS Viterbi decoding. This modulation and coding scheme also provides the highest bit error rate performance of all the schemes described in SMAD [15]. The one downside is this scheme is computationally complex. Based on Figure 4.3, if a system requires a small diameter antenna, a

scheme that uses Viterbi decoding is most beneficial. However, if size of the antenna is not an issue, a computationally simpler scheme that does not use Viterbi decoding is likely more beneficial.

4.6   Communications Subsystem Summary

For the mass driver communications subsystem, a single antenna will be used alongside a diplexer for both transmitting and receiving data from an Earth ground station and a lunar colony. The antenna diameter will be 1.5 m, which when combined with a binary phase shift keying scheme and RS Viterbi decoding will require 4.27 W during transmission to an Earth ground station and require $8.99e^{-9}$ W during transmission to a lunar colony.

To accommodate for unexpected rain attenuation or other adverse atmospheric conditions, the electrical power subsystem will be designed to provide up to 5 W to the communications subsystem.

5. Thermal Control Subsystem

5.1   Requirements

The requirements for the thermal control subsystem (TCS) outlined in chapter 2 are:

- The thermal control subsystem shall maintain an operational temperature less than 400 K across the entire mass driver.
- The thermal control subsystem shall maintain an operational temperature between 233 K and 343 K for the control electronics.

The mass driver can be broken down into an accelerating section and a decelerating section. Each section is further broken down into nearly identical 2 m long modules which contain the superconductors and driver coils accelerating the payload. Since the modularity of the mass driver improves adaptability, the thermal load will be examined for an individual module and then multiplied by the number of modules.

For each module, the key temperature requirements are:

- The temperature shall not exceed an operational temperature of 400 K in the hot case.
- The temperature shall not drop below an operational temperature of 250 K in the cold case.
- The temperature shall not drop below a survival temperature of 233 K in the non-operational cold case.

The control electronics shall be housed in a thermally controlled environment that meets the operational temperature requirements outlined at the beginning of this chapter.

5.2   Environmental Loading

During the literature review it was identified that the lunar poles would make an ideal location for a mass driver due to being in sunlight approximately 80% of the time. With this in mind, it is assumed that 80% of a normal 24-hour day will be spent in constant sunlight while the remaining 20% of a normal 24-hour day will be spent in darkness.

Since the mass driver will be located on the moon, certain environmental heat sources traditionally present in spacecraft design will be assumed to be negligible, including infrared (IR) from the Earth and albedo radiation from the Earth. However, while the Earth's IR heating effects can be ignored, the moon's IR heating effects cannot, and will be one of the two major environmental loads placed on the TCS.

The TCS will be designed around the two extreme temperature conditions the mass driver is expected to experience. First is the hot case, when all the electronics are in use, the superconductors are producing their maximum waste heat, and the mass driver is in direct sunlight while the moon is closest to the sun. Next is the cold case, when all the electronics are off, the mass driver is not operational, and there is no direct sunlight on the mass driver.

5.3 Thermal Control Options

A number of thermal control options are available for the mass driver. Ideally, the TCS will be composed of entirely passive thermal control elements to minimize the power requirement for the TCS. The main passive thermal control elements are radiators, multilayer insulation, and surface finishes. One other method of passive thermal control is the use of heat pipes, but due to the Moon's gravity, simple capillary heat pipes would be ineffective. To make heat pipes work while under the influence of the Moon's gravity, more complex and expensive Loop heat pipes would likely be required [15].

While passive thermal control elements may be sufficient for keeping the mass driver below the required maximum operating temperature during the hot case, active heating elements may be required to keep the mass driver above the minimum survival temperature during the cold case. If active heating elements are required, the simplest options are patch or cartridge heaters. Between these options, patch heaters are preferrable as they are reusable and more easily controllable via thermostat.

5.4 Radiator Sizing

The governing equations for the design of a passive thermal control system are outlined in SMAD [15] and shown below:

$$q_{external}A + Q_{internal} = Q_{radiator} \tag{5.1}$$
$$Q_{radiator} = \varepsilon\sigma AT^4 \tag{5.2}$$

First, the radiator area required to keep the mass driver below maximum operating temperature will be calculated. During the radiator sizing process, a 10 K uncertainty margin will be used to account for differences between theory and application. This set of calculations will assume that the radiators used for the TCS will be finished with 5 mil aluminized Teflon to provide low absorptivity and high emissivity, while not being as expensive as a silver finish. In a later section, the effects of various radiator surface finishes outlined in SMAD [15] on the radiator area will be analyzed.

Table 5.1 shows the values used in the radiator sizing calculations for the hot case and cold case for each mass driver module.

Table 5.1- Radiator sizing input parameters

Parameter	Hot Case	Cold Case
Solar Constant	1420 W/m^2	1360 W/m^2
Moon IR	430 W/m^2	430 W/m^2
Solar Absorptance	0.2	0.1
IR Emittance	0.72	0.78
Power Dissipation	5620 W	0 W

With these values, the radiator size for each module for the hot case can be determined using rearranged equations from SMAD [15]:

$$A = \frac{Q_{int}}{\sigma \varepsilon T^4 - q_{ext}}$$

$$= \frac{5620\ W}{\left(5.67 * 10^{-8} \frac{W}{m^2 K^4}\right)(0.72)(400\ K)^4 - \left(430 \frac{W}{m^2} + 1420 \sin(5°)\ W/m^2\right)} \quad (5.3)$$

$$= 11.4\ m^2$$

For a 2 m long module, 11.4 m² is a large, required radiator area. This area could be reduced by up to 9% if the radiators could be placed in a location which received no sunlight, but that still results in a large area of 9.14 m². If Loop heat pipes are utilized to evenly distribute the heat across the radiator surface, the required radiator area could be further reduced.

With the required radiator area calculated, the amount of heater power required during the cold case can be determined using equations from SMAD [15]:

$$Q_{int} = \sigma \varepsilon A T^4 - q_{ext} A$$

$$= \left(5.67 * \frac{10^{-8} W}{m^2 K^4}\right)(0.78)(11.4\ m^2)(233\ K)^4 \quad (5.4)$$

$$+ -\left(430 \frac{W}{m^2}\right)(11.4\ m^2) = -3420\ W$$

The resulting negative number indicates that heater power is not required to keep the mass driver and electronics above the non-operational survival temperature of 233 K, which also means the thermal system can be entirely passive.

5.5 Thermal Control Analysis

While the calculations in the previous section assume a 5 mil aluminized Teflon radiator surface finish, there are additional surface finishes listed in SMAD [15] which have different emissivity. MATLAB code used to examine the effects of other surface finishes can be found in Appendix B and is based on the calculations performed in the previous section. One of the things displayed in Figure 5.1 is the effect of different surface finishes on the required radiator surface area.
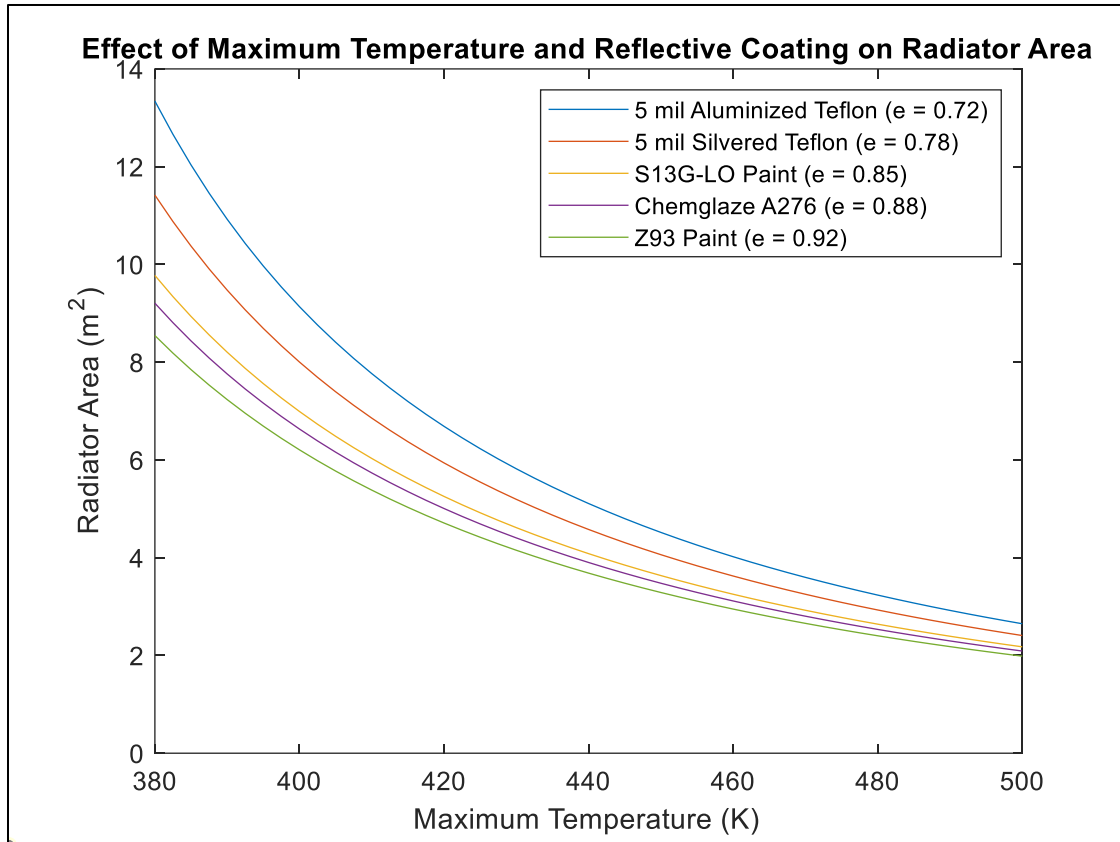
Figure 5.1- Effect of maximum temperature and surface finish on radiator area

Figure 5.1 shows that a higher emissivity results in a lower required radiator area which makes intuitive sense. Specifically, a Z93 white paint surface finish results in the lowest required radiator area to keep the mass driver below the required maximum operating temperature with an area of 6.2 m^2.

The other relationship displayed in Figure 5.1 is the relationship between radiator area and maximum system temperature. As the maximum allowable operating temperature increases, the required radiator area decreases, but there appears to be diminishing returns as the temperature is continually increased. This indicates that if the maximum allowable operating temperature for the mass driver could be increased, the radiator area could be reduced, resulting in potential weight savings.

Since the maximum allowable operating temperature affects the required radiator area, the maximum operating temperature also affects the required heating power during the cold case. Figure 5.2 displays the relationship between the two variables and shows the effect of various radiator surface finishes. In all cases, the required heater power is negative, indicating that the mass driver will stay above the minimum survival temperature without requiring active heating in all the examined scenarios.
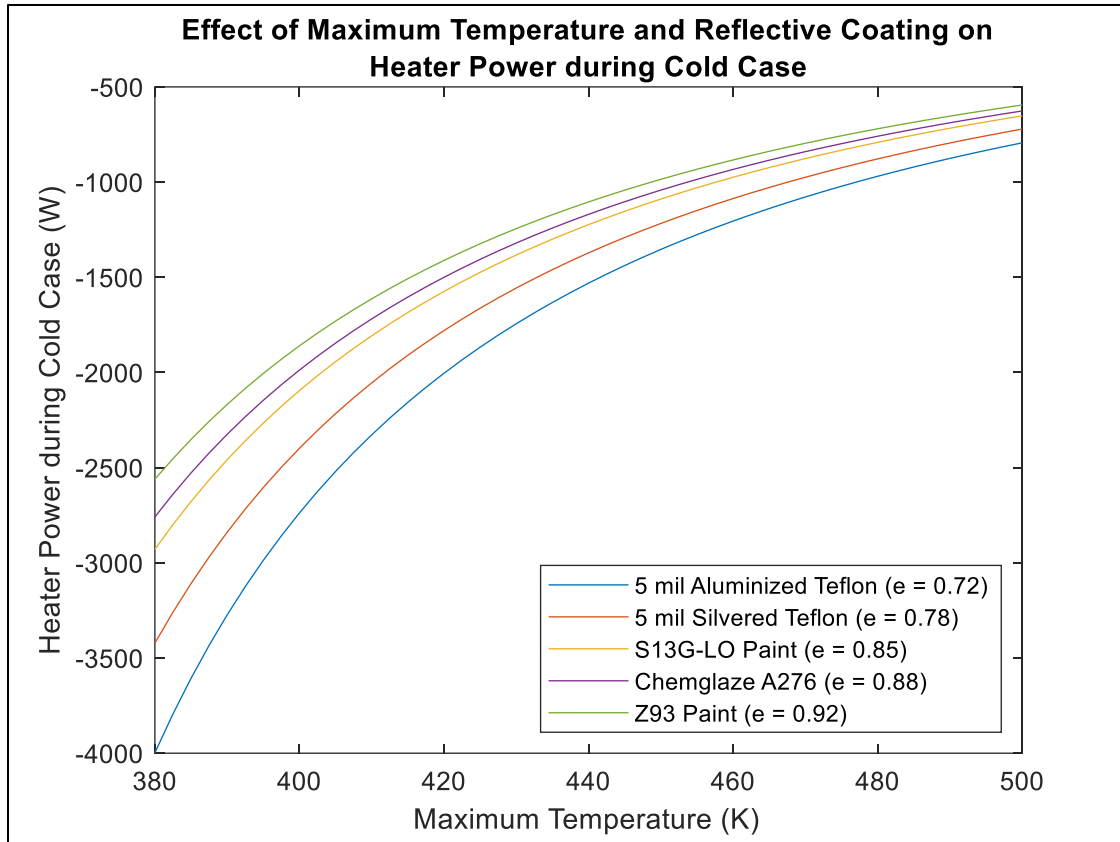
Figure 5.2- Effect of maximum temperature and surface finish on heater power

5.6 Thermal Control Summary

The primary element of the thermal control subsystem will be radiators with a Z93 white paint finish. Loop heat pipes will also be used to optimize the effectiveness of the radiators. While not explicitly necessary, additional electrical resistance patch heaters will be added to the mass driver to raise the system temperature in the event of emergency. The entire TCS will be controlled by a solid-state temperature controller that is linked to mechanical temperature sensors in each mass driver module. Each 2 m long module will have approximately 6.2 m^2 of radiators to dissipate the waste heat generated by the mass driver superconducting coils.

While the calculations were performed assuming a 5°sunlight incidence angle on the radiators, it is recommended that the radiators should be placed such that they are almost never in sunlight as this can further reduce the required radiator area by upwards of 9%. Additionally, in the future, further TCS analysis and optimization specifically regarding the placement and utilization of Loop heat pipes should be able to further reduce the required radiator area. However, until that advanced analysis is performed, it is impossible to know how effective the Loop heat pipes will be.

The primary TCS is passive and does not require any power to keep the superconducting coils and control electronics within operational temperatures. However, approximately 100 W will be dedicated during the electrical power subsystem design to power the resistance patch heaters in the event of emergency.

6. Electrical Power Subsystem

6.1   Requirements

The requirements for the electrical power subsystem (EPS) outlined in chapter 2 are:

- The power subsystem shall provide at least 8.7 MW to the mass driver while the mass driver is operational.
- The power subsystem shall provide enough power to operate the active component of the thermal control subsystem.
- The power subsystem shall provide enough power to operate the communications subsystem.

Based on the calculations performed in chapters 4 and 5, the required power for both the TCS and communications subsystems is known. Specifically:

- The EPS shall provide 100 W to the thermal control subsystem in the event of emergency, during an eclipse cold case.
- The EPS shall provide 5 W to the communications subsystem during uplink or downlink with Earth or a lunar colony.

These power requirements are small relative to the power requirement for the mass driver but are integral to the design of the energy storage system during eclipse. The other requirement of importance is the mission life of 20 years, as this affects the options available during the design of the EPS.

6.2   Power Source Selection

The combination of long mission life and a high power output makes power source selection difficult. SMAD presents a table comparing five of the traditional power sources used for space missions and a copy of that table is shown below [15]:

Table 6.1- Comparison of traditional space mission power sources according to SMAD [15]

EPS Design Parameters	Solar Photovoltaic	Solar Thermal Dynamic	Radioisotope	Nuclear Reactor	Fuel Cell
Power Range (kW)	0.2-300	5-300	0.2-10	5-300	0.2-50
Specific Power (W/kg)	25-200	9-15	5-20	2-40	275
Hardness -Natural Radiation -Nuclear Threat	Low-Medium Medium	High High	Very High Very High	Very High Very High	High High
Degradation Over Life	Medium	Medium	Low	Low	Low
Sensitivity to Sun Angle	Medium	High	None	None	None
Fuel Availability	Unlimited	Unlimited	Very Low	Very Low	Medium
Safety Analysis Reporting	Minimal	Minimal	Routine	Extensive	Routine

Traditional photovoltaics and nuclear radioisotope power sources are considered static power sources. The advantage of these systems is the relative simplicity compared to a dynamic power source. A static power source directly generates electricity, while a dynamic power source uses generated heat to power a Rankine, Brayton, or Stirling cycle which then in turn produces electricity. The advantage of dynamic power sources is they usually have a greater specific power and a higher power range than static power sources.

Table 6.1 shows that none of the traditional space mission power sources have been used to produce the power required by the mass driver. The power sources that are closest are solar photovoltaics, solar thermal dynamic, and a nuclear reactor. Of these sources, the most expensive and potentially the most dangerous is a nuclear reactor. The nuclear reactor requires extensive and constant safety reporting, extremely high levels of radiation hardness, and the continual threat of nuclear meltdown. When combined with the difficulty of scaling up the power generated with the potential litany of political ramifications, a nuclear reactor is not a viable candidate for power generation for the mass driver.

The remaining two options both involve solar, but harness it in different ways. Photovoltaics directly convert solar energy into electricity, and scaling up the power generated is largely a matter of building a bigger array of solar panels. A solar thermal dynamic system on the other hand uses solar energy to provide heat for a Stirling, Rankine, or Brayton cycle. Scaling up a solar thermal dynamic system would require either larger Stirling, Rankine, or Brayton engines, or a larger number of smaller engines.

In either case, the process of dynamic power generation has a higher likelihood of failure than photovoltaics due to the high working temperatures and pressures involved in Brayton, Rankine,

and Stirling engine systems. Due to this, photovoltaics will be the power source utilized for this project. The specific type of photovoltaic will be determined following an analysis of the power generation capabilities of various types of solar panels in a later section. In the following sections, a preliminary calculation of solar array size and battery capacity will be performed assuming indium-phosphide solar cells.

6.3   Solar Array Sizing

The solar array will be located away from the mass driver to eliminate any shadowing or electrical interference effects. This will also provide more room for the solar array to fully utilize sun-tracking sensors, optimizing energy production.

For the purposes of determining time in eclipse and time in sunlight, it will be assumed that in a 24-hour normal day, the solar array will be in sunlight 80% of the time. Additionally, due to the high power requirements of the mass driver, the mass driver will not be operated during eclipse leaving only the communications and TPS subsystems potentially active. This results in the values in Table 6.1 below:

Table 6.2 - Eclipse and sunlight requirements

	Eclipse	Sunlight
Time	4.8 hours	19.2 hours
Power Required	105 W	8.7 MW
Path Efficiency	0.65	0.85

Utilizing the above values and equations from SMAD [15], the required solar array power can be calculated:

$$P_{sa} = \frac{(\frac{P_{ec}T_{ec}}{X_{ec}} + \frac{P_{dl}T_{dl}}{X_{dl}})}{X_{dl}} = \frac{(\frac{(105\ W)(4.8\ hr)}{0.65} + \frac{(8.7 * 10^6\ W)(19.2\ hr)}{0.85})}{19.2\ hr} \tag{6.1}$$
$$= 10.3 * 10^6\ W = 10.3\ MW$$

Next the beginning of life and end of life power of the solar array per unit area must be determined:

$$P_{BOL} = P_o I_{dg} cos\theta = (0.228)\left(1367\frac{W}{m^2}\right)(0.77)\cos(30°) = 208\ W/m^2 \tag{6.2}$$
$$L_{dg} = (1 - degradation/year)^{satellite\ life} = (1 - 0.015)^{20} = 0.739 \tag{6.3}$$
$$P_{EOL} = P_{BOL}L_{dg} = \left(208\frac{W}{m^2}\right)(0.739) = 154\ W/m^2 \tag{6.4}$$

Finally, the area of the solar array can be calculated:

$$A_{sa} = P_{sa}/P_{EOL} = \frac{10.3 * 10^6 \, W}{154 \frac{W}{m^2}} = 67000 \, m^2 \tag{6.5}$$

To successfully power the mass driver, based on the solar array area calculated above, a 260 m square solar array will be required. The size of the solar array may seem staggering compared to the size of solar arrays powering traditional satellites. However, research performed in solar collection satellites which propose solar array sizes of nearly 5 km^2 [16] indicate that the size of solar array required to power the mass driver is actually feasible. Additionally, it is possible that solar cells made of a material other than indium-phosphide may result in a smaller and more efficient solar array. This possibility will be examined in a later section.

6.4   Energy Storage

While the solar array required is large, since the mass driver will not be operating during eclipse, the energy storage system will be much smaller. Due to the long mission life, two batteries will be used, but the batteries will be redundant and not used in series or parallel, so each battery must individually provide enough power during eclipse.

The required battery capacity is calculated using equations from SMAD [15]:

$$C_b = \frac{P_{ec}T_{ec}}{(DOD)Nn} = \frac{(105 \, W)(4.8 \, hr)}{(25\%)(1)(0.9)} = 2240 \, W * hr \tag{6.6}$$

The specific type of battery does not need to be specified for the energy storage calculation, but the effect of the material on energy storage mass will be examined in the next section.

6.5   Solar Array and Energy Storage Analysis

In the previous sections, specific materials were selected from ones outlined in SMAD [15], however materials science and engineering have advanced since SMAD was published. The materials outlined in SMAD will be compared to newer materials to determine if there is a potential benefit to using the newer materials and technology. Table 6.3 shows different solar panel types and their respective efficiencies and rates of degradation while Figure 6.1 shows a comparison of different solar panel types and the resulting effect on the required solar array as a function of solar incidence angle.

Table 6.3 - Efficiency and rate of degradation for various solar panel types

Solar Panel Type	Efficiency	Rate of Degradation (per year)
Silicon [15]	20.8%	1.61%
Gallium Arsenide [15]	21.8%	0.49%
Indium-Phosphide [15]	19.9%	0.10%
Multijunction GaAs [15]	25.7%	0.49%
Emcore ATJ [17]	28%	1.08%
Multijunction GaInP/GaAs/GaInAs [18]	35.8%	1.35%
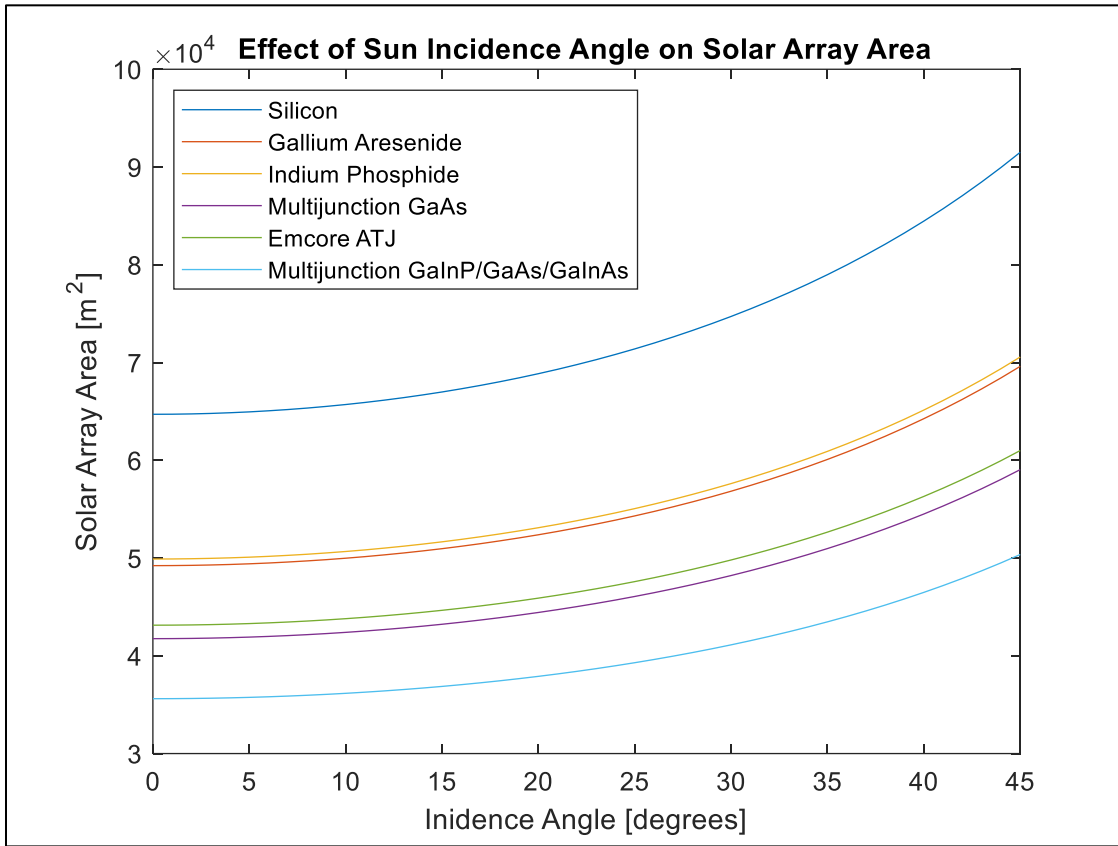
Figure 6.1- Effect of sun incidence angle and solar panel material on solar array area

Interestingly, each of the solar panel types stays within the same order of magnitude for the required solar array area, regardless of the efficiency. One potential exception to this observation is the experimental multijunction GaInP/GaInAs panels which despite having the second highest rate of degradation, resulted in the smallest solar array area. This indicates that the relatively large jump in efficiency more than makes up for the high rate of degradation. If in the future, this type of multijunction solar panel can be made to have a reduced rate of degradation, the area savings would be substantial, as shown in Figure 6.2.
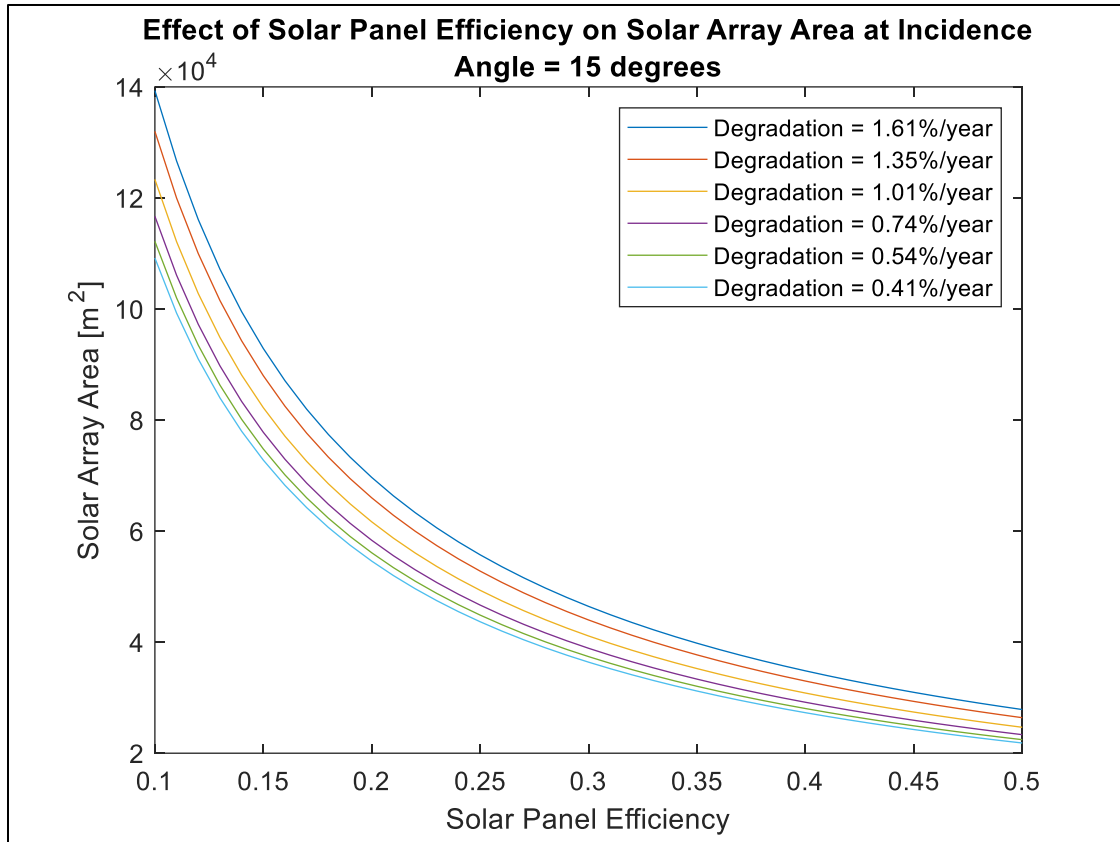
Figure 6.2 - Effect of solar panel efficiency on solar array area at incidence angle of 15°

Based on Figure 6.2, even bringing the rate of degradation for GaInP/GaInAs multijunction panels from the current rate of 1.35% per year to the GaAs 0.49% per year would result in a substantial reduction in solar array area. Specifically, it results in an area reduction of approximately 15% which is significant.

$$\left| \frac{37,710 \ m^2 - 32,054 \ m^2}{37,710 m^2} \right| * 100\% = 15\% \tag{6.7}$$

Also of note, based on Figure 6.1 for small angles up to about 15° the incidence angle has a small effect on the overall size of the solar array. Specifically, the change in solar array area from 0° to 15° is approximately 3.53%.

$$\left| \frac{35,612 \ m^2 - 36,868 \ m^2}{35,612 \ m^2} \right| * 100\% = 3.53\% \tag{6.8}$$

However, beyond 15° the incidence angle starts having a notable negative impact on the solar array size. Specifically, the change in solar array area from 15° to 30° is approximately 11.53%

$$\left| \frac{36{,}868 \; m^2 - 41{,}121 \; m^2}{36{,}868 \; m^2} \right| * 100\% = 11.53\% \tag{6.9}$$

Since the solar array is apart from the mass driver, sun tracking and solar array pointing systems can be used to minimize power loss from high incidence angles, with the goal of keeping the worst-case incidence angle below 15°.

The two main types of batteries used for energy storage in space applications are nickel-cadmium and nickel-hydrogen batteries. Both have been extensively tested in the space environment and used aboard numerous spacecraft, including the International Space Station (ISS) [19]. However, lithium-ion batteries have begun to be experimented with aboard spacecraft and provide a sizeable increase in specific energy density. According to the NASA team involved in the design of the ISS EPS, a single lithium-ion battery of identical size and weight to a previously designed nickel-hydrogen battery had more than double the energy density [19]. Table 6.4 shows the mass of the energy storage system for the three common types of batteries [15].

Table 6.4 - Battery specific energy density and mass

Battery Type	Specific Energy Density (W*hr/kg)	Battery Mass (kg)
Nickel-Cadmium [15]	25-30	75-90
Nickel-Hydrogen [15]	43-57	39-52
Lithium-Ion [15, 18]	70-140	16-32

6.6 Power Regulation Considerations

For the regulation of power from the solar array to the mass driver system, a direct-energy-transfer (DET) control subsystem will be used. The DET subsystem is better suited to the long mission life and constant power requirement of the mass driver than the alternative peak-power tracker subsystem. Additionally, the DET subsystem will not require a sizeable portion of the solar array's power to function, increasing the system efficiency of the solar array.

Since the mission life is more than 5 years, an unregulated bus subsystem will be utilized in conjunction with independent chargers for the batteries. The independent chargers should improve battery life, and the unregulated system will be more power efficient than a fully or quasi regulated system.

6.7 Electrical Power Summary

The power requirements for the mass driver are high and as a result a large solar array is required to supply the necessary energy. Fortunately, while the solar array is large, the battery capacity is comparatively smaller. This is due to the mass driver not being operational during eclipse.

A solar array of approximately 37,000 m^2 composed of multijunction GaInP/GaInAs panels with a solar incidence angle of 15° or less will be used to power the mass driver. An energy storage system holding 2,240 W*hr in two redundant lithium-ion batteries with a mass of approximately 16 kg will be used to power the communications subsystem and an emergency heating system during eclipse. The EPS is controlled using a direct-energy-transfer control subsystem and an unregulated bus subsystem will be utilized to increase battery life and overall power efficiency.

In the future, it is suggested that a closer look be taken at a nuclear reactor as a potentially viable energy source for the mass driver. A nuclear reactor would ideally not take up as much space as the required solar array and would not be contingent on sunlight, increasing the amount of operational time for the mass driver. At this time, there is not enough research into the implementation of a nuclear reactor on the lunar surface for the idea to be fully analyzed or considered.

7. Orbital Trajectory Analysis

7.1   Initialization and Assumptions

In addition to the design of the mass driver subsystems, the orbital trajectory of the payload must be analyzed. One of the requirements for the mass driver is that it delivers the payload to LEO, so the mass driver must be designed to accomplish this task. Since the magnitude of the exit velocity of the payload was determined in Chapter 3, the magnitude of the exit velocity is not a variable that can be changed to manipulate the orbital trajectory of the payload. What can be manipulated, during the design process, is the exit velocity vector.

The mass driver will be built at the lunar northern pole for the reasons outlined in Chapter 1. Since the Moon orbits the Earth at approximately the same speed the Moon rotates about its axis, a mass driver built at the lunar northern pole will always point toward Earth, with minimal variance in angle. This means that the mass driver can be built at whatever angle results in a payload trajectory that reaches LEO in the shortest possible amount of travel time.

To determine the optimal payload trajectory, a circular planar restricted three-body problem approach will be utilized. A three-body problem approach will be utilized as both the Moon and the Earth have noticeable gravitational effects on the payload during the payload orbit, and neglecting either celestial body would result in erroneous results. The mass of the payload is negligible when compared to the mass of the Moon and of the Earth, which means the three-body problem is restricted. The circular and planar assumptions simplify the problem further by ignoring the small eccentricity of the Moon's orbit around the Earth, and by keeping the problem planar, enabling the three-body problem to be solved.

The methodology and approach utilized for this circular planar restricted three-body problem will be taken from Hunter's Astrodynamics Course Reader [20]. First a non-Newtonian reference frame is defined, called the Barycenter frame. The origin of the Barycenter frame is defined as the center of mass of the Earth-Moon system. The x-axis of the Barycenter frame is defined as the line that joins the Earth and the Moon, while the y-axis is defined so that both the x-axis and y-axis are on the ecliptic plane, and the z-axis is perpendicular to the ecliptic plane.
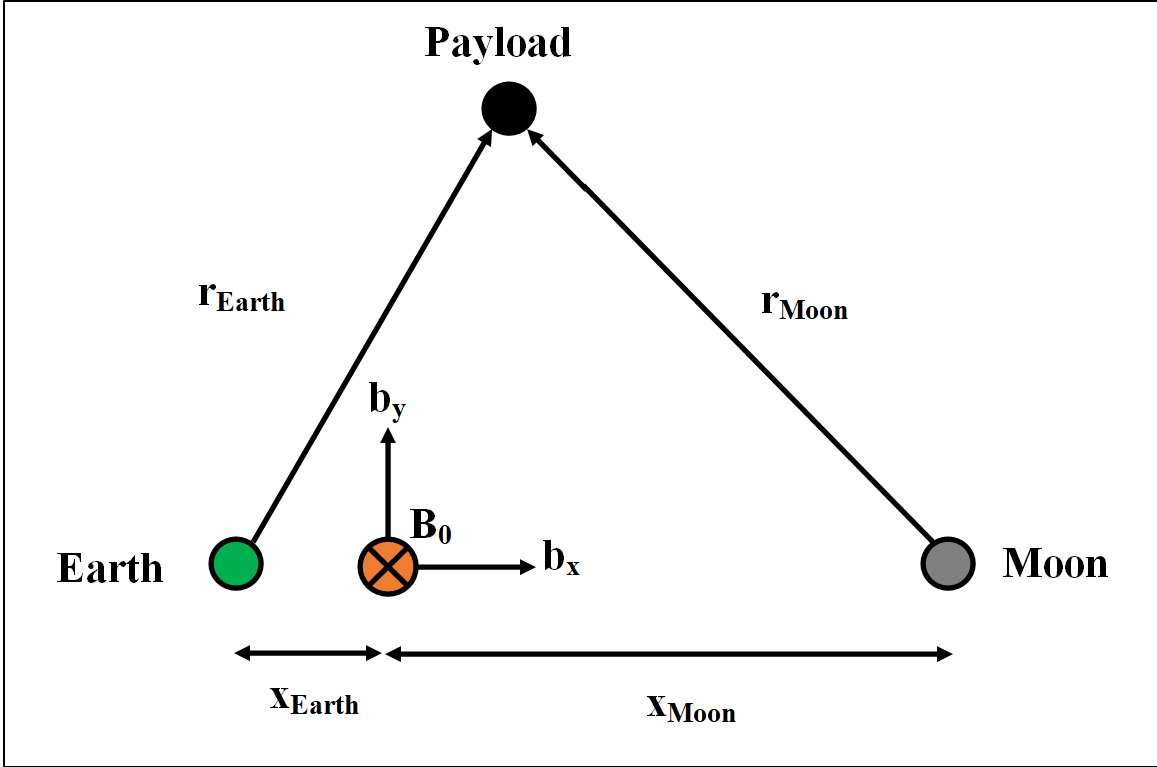
Figure 7.1- Planar Barycenter Frame for Restricted Three-Body Problem

Next, the angular velocity of the Barycenter frame with respect to the Newtonian reference frame is defined:

$${}^{S}\boldsymbol{\omega}^{B} = \omega\ \mathbf{b}_{z} \tag{7.1}$$

The magnitude of the angular velocity is constant and is directly related to the orbital period, τ, of the Earth-Moon system around the Barycenter.

$$\omega = \frac{2\pi}{\tau} \tag{7.2}$$

$$\tau = \frac{2\pi}{\sqrt{G(M_{ea} + M_m)}}\, r_{em}^{3/2} \tag{7.3}$$

$$\omega = \frac{\sqrt{G(M_{ea} + M_m)}}{r_{em}^{3/2}} \tag{7.4}$$

The final element of the definition of the Barycenter is the position of the Barycenter, relative to the Earth and the Moon. Since the Barycenter is defined as the location of the center of mass of the Earth-Moon system, the location of the center of mass must be determined. The following two relations will be used to calculate the distance between the Barycenter and the Earth, and the distance between the Barycenter and the Moon:

$$-M_{ea}x_{ea} + M_m x_m = 0 \tag{7.5}$$
$$r_{em} = x_{ea} + x_m \tag{7.6}$$

Substituting equation 7.5 into equation 7.6 results in:

$$x_{ea} = r_{em}\frac{M_m}{M_{ea} + M_m} = (384{,}400 \ km)\frac{7.347 * 10^{22} \ kg}{(5.972 * 10^{24} \ kg + 7.347 * 10^{22} \ kg)} \\ = 4{,}672 \ km \tag{7.7}$$

The Barycenter is located approximately 4,672 km from the center of the Earth, or almost 75% of the radius of the Earth. This makes sense since the Earth is almost two orders of magnitude more massive than the Moon.

7.2   Equations of Motion

With the Earth-Moon Barycenter defined, the equations of motion for the payload can be derived. The acceleration of the payload in the Newtonian reference frame, combined with the constant magnitude angular momentum of the Barycentric frame, is:

$${}^S\mathbf{a}^Q = {}^B\mathbf{a}^Q + {}^S\boldsymbol{\omega}^B \times ({}^S\boldsymbol{\omega}^B \times {}^B\mathbf{r}^Q) + 2*{}^S\boldsymbol{\omega}^B \times {}^B\mathbf{v}^Q \tag{7.8}$$

The acceleration can be expanded into the Barycentric frame, resulting in:

$${}^S\mathbf{a}^Q = \ddot{x}\boldsymbol{b}_x + \ddot{y}\boldsymbol{b}_y + \ddot{z}\boldsymbol{b}_z + \left(\omega\boldsymbol{b}_z \times \left[\omega\boldsymbol{b}_z \times (x\boldsymbol{b}_x + y\boldsymbol{b}_y + z\boldsymbol{b}_z)\right]\right) + (2\omega\boldsymbol{b}_z \times [\dot{x}\boldsymbol{b}_x + \\ \dot{y}\boldsymbol{b}_y + \dot{z}\boldsymbol{b}_z]) \tag{7.9}$$
$$= (\ddot{x} - 2\omega\dot{y} - \omega^2 x)\boldsymbol{b}_x + (\ddot{y} + 2\omega\dot{x} - \omega^2 y)\boldsymbol{b}_y + (\ddot{z})\boldsymbol{b}_z \tag{7.10}$$

The only force acting upon the payload in this problem is gravity. Specifically, the only two sources of gravity being considered in this restricted three-body problem are the Earth and the Moon. Using Newton's 2nd law, the equations of motion for the payload can now be determined.

$$\frac{-GM_{ea}m}{r_{ea}^2}\boldsymbol{u}_{r_{ea}} - \frac{GM_m m}{r_m^2}\boldsymbol{u}_{r_m} = m\,{}^S\mathbf{a}^Q \tag{7.11}$$

$$\frac{-GM_{ea}m}{r_{ea}^2}\boldsymbol{u}_{r_{ea}} - \frac{GM_m m}{r_m^2}\boldsymbol{u}_{r_m} \\ = m[(\ddot{x} - 2\omega\dot{y} - \omega^2 x)\boldsymbol{b}_x + (\ddot{y} + 2\omega\dot{x} - \omega^2 y)\boldsymbol{b}_y + (\ddot{z})\boldsymbol{b}_z] \tag{7.12}$$

Next the gravitational force vectors must be converted to Barycentric vectors:

$$\boldsymbol{u}_{r_1} = \frac{\boldsymbol{r}_{ea}^{Payload}}{|\boldsymbol{r}_{ea}^{Payload}|} = \frac{\left(x + \dfrac{M_m}{M_{ea} + M_m}r_{em}\right)\boldsymbol{b}_x + y\boldsymbol{b}_y + z\boldsymbol{b}_z}{r_{ea}} \tag{7.13}$$

$$u_{r_2} = \frac{r_m^{Payload}}{|r_m^{Payload}|} = \frac{\left(x - \frac{M_{ea}}{M_{ea} + M_m} r_{em}\right) b_x + y b_y + z b_z}{r_m} \tag{7.14}$$

Substituting the resulting vectors into equation 7.12 and separating the equation into scalar components results in the following equations of motion:

(b_x)
$$\ddot{x} - 2\omega\dot{y} - \omega^2 x = -\frac{GM_{ea}}{r_{ea}^3}\left(x + \frac{M_m}{M_{ea} + M_m} r_{em}\right) - \frac{GM_m}{r_m^3}\left(x - \frac{M_{ea}}{M_{ea} + M_m} r_{em}\right) \tag{7.15}$$

(b_y) $\ddot{y} + 2\omega\dot{x} - \omega^2 = (\frac{-GM_{ea}}{r_{ea}^3} - \frac{GM_m}{r_m^3})y$ $\tag{7.16}$

(b_z) $\ddot{z} = (-\frac{GM_{ea}}{r_{ea}^3} - \frac{GM_m}{r_m^3})z$ $\tag{7.17}$

Equations 7.15 and 7.16 are coupled, indicating that a numerical approach will be required to solve the equations of motion in the x and y directions. The z direction, however, is independent of both the x and y directions, meaning that if the payload begins in planar motion, as assumed, the payload will remain in planar motion. This indicates that equation 7.17 should not be needed for this orbital analysis.

7.3   Methodology

Since equations 7.15 and 7.16 are coupled, MATLAB will be utilized to provide a numerical solution. Specifically, the function ode45 will be used. The initial conditions used to solve the equations of motion will be the x and y positions of the payload at the instant it is launched from the mass driver, and the magnitude of the mass driver exit velocity in the x and y directions.

The magnitude of the mass driver exit velocity was determined in Chapter 3 and will not be changed. Rather, the angle of the mass driver will be changed, ranging from -60° to 60° from the Barycentric x-axis and rotating about the Barycentric z-axis, to provide a series of potential orbital trajectories. From the resulting trajectories, the trajectory that reaches LEO in the shortest time, and that does not result in an impact with the Earth, will be selected. The MATLAB code utilized can be found in Appendix B.

7.4   Results and Analysis

7.4.1   MATLAB Data

Across the -60° to 60° spectrum, only a narrow range of angles produced an orbital trajectory which brought the payload within LEO. The specific range of angles which produced an orbital trajectory bringing the payload within LEO, and the corresponding time required to reach LEO can be seen in Table 7.1.

Table 7.1- Time required to reach GEO, LEO, and Earth for a given launch angle

Angle (°)	Time to GEO (days)	Time to LEO (days)	Time to Earth (days)
20	1.7475	2.1786	2.224
21	1.6391	1.9841	2.1567
22	1.5615	1.808	1.8586
23	1.3647	1.7966	1.8311
24	1.2128	1.4121	1.4121
25	----	----	----
26	0.9607	1.1391	1.1666
27	1.2414	1.5292	1.5832
28	1.3228	1.8739	1.9658
29	1.4941	1.915	1.9571
30	1.6113	2.0198	2.0652
31	1.7484	2.1424	----

As can be seen in Table 7.1, only a single angle, 31°, results in the payload passing through LEO without eventually impacting Earth. The absence of data for 25° is due to an apparent singularity during the numerical solution process. While MATLAB did produce values, MATLAB also produced warnings indicating a singularity had occurred and that the result would likely be inaccurate. The results produced by MATLAB for the 25° case were several orders of magnitude off from the other results and did not make physical sense.

7.4.2   Partial Solutions

As discussed in Section 7.4.1, only a mass driver launch angle of 31° results in a complete solution. However, it is important to note that while the 20° to 30° range of angles results in an eventual impact with Earth, theoretically an orbital facility capturing the payload could be placed in a location which would intercept the payload before it would impact Earth. This means that these additional launch angles provide potential alternatives, should an alternative angle be necessary.

Shown in Figures 7.2 through 7.5 are several partial solutions with trajectories that reach LEO, but that also eventually result in an impact with the Earth.
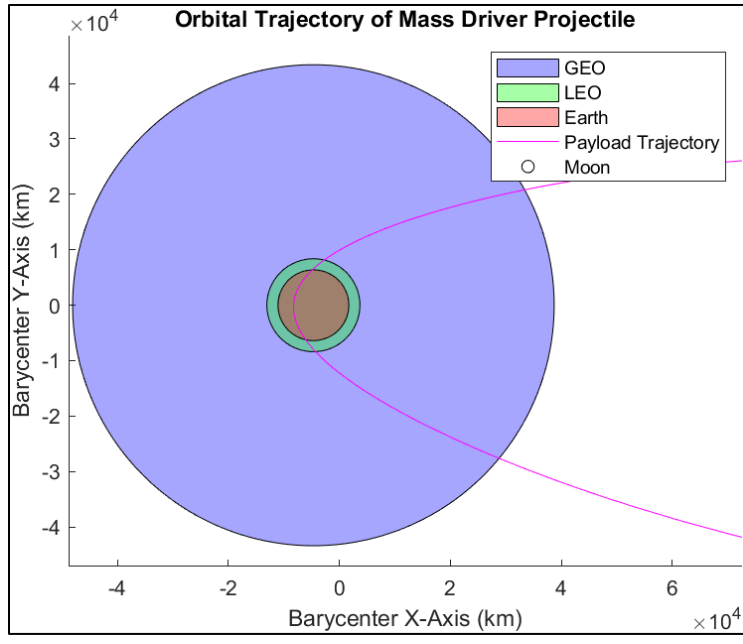
Figure 7.2- Close-up of orbital trajectory of payload launched at 21°
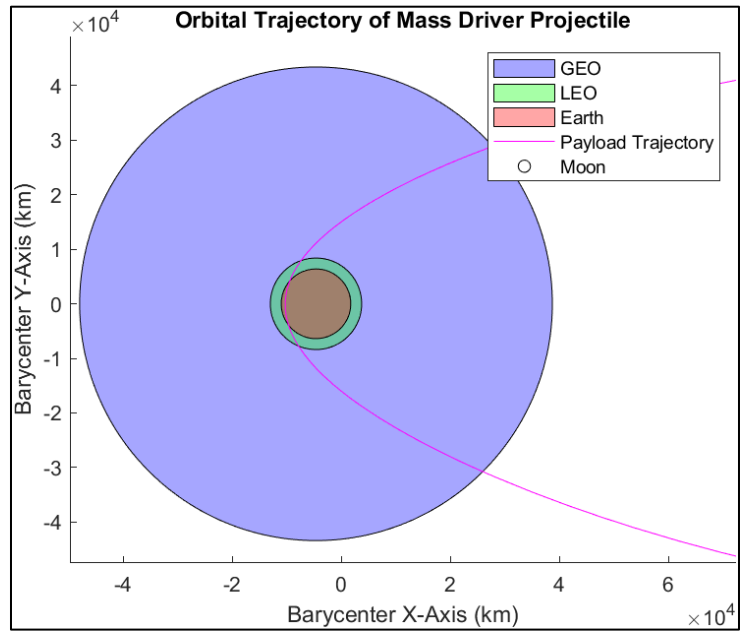

Figure 7.3- Close-up of orbital trajectory of payload launched at 22°
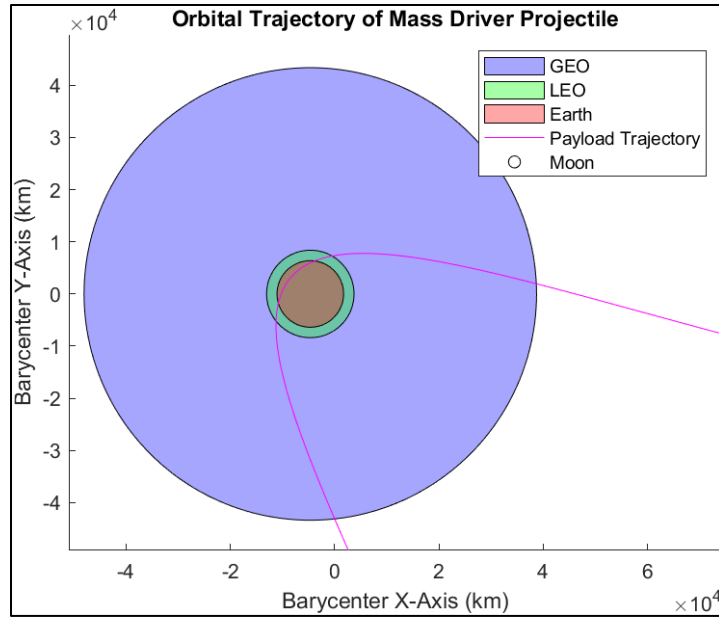
Figure 7.4- Close-up of orbital trajectory of payload launched at 30°
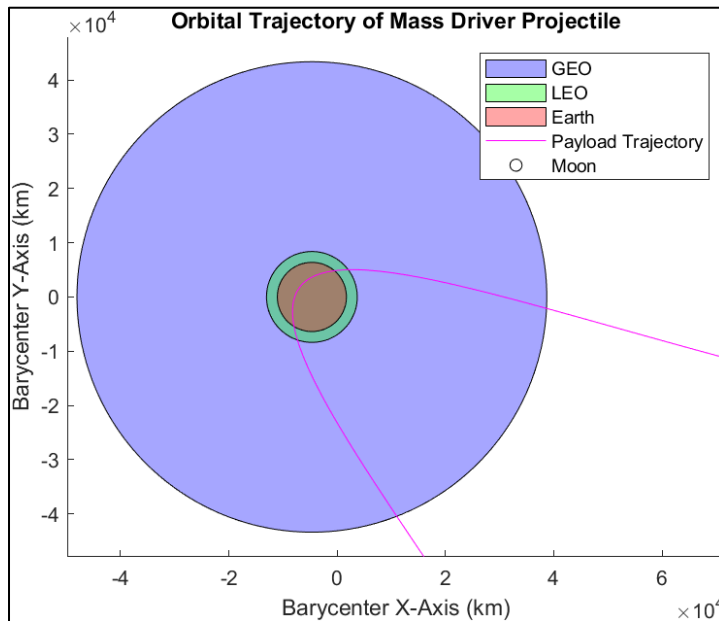
Figure 7.5- Close-up of orbital trajectory of payload launched at 29°

7.4.3   Complete Solution

The single complete solution for a mass driver launch angle that results in a trajectory passing through LEO while not impacting the Earth is an angle of 31°. Figure 7.6 displays the resulting payload trajectory as it leaves the lunar surface and eventually passes through LEO. As can be seen, if the payload is not intercepted while in LEO, the payload will eventually begin a return trajectory back toward the Moon. Figure 7.7 shows a close-up of the payload passing through LEO.

40

Figure 7.6- Orbital trajectory of payload at 31°

Figure 7.7- Close-up of orbital trajectory of payload at 31° as the payload passes LEO

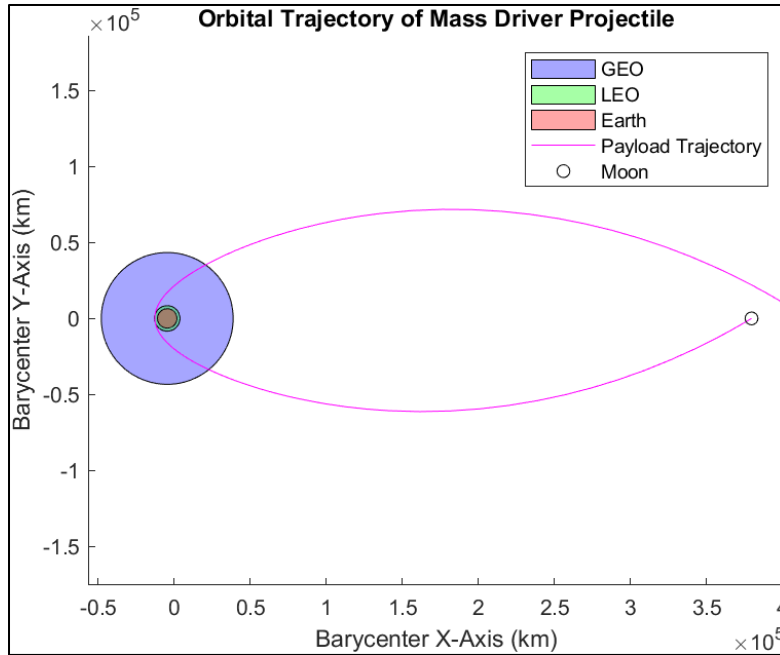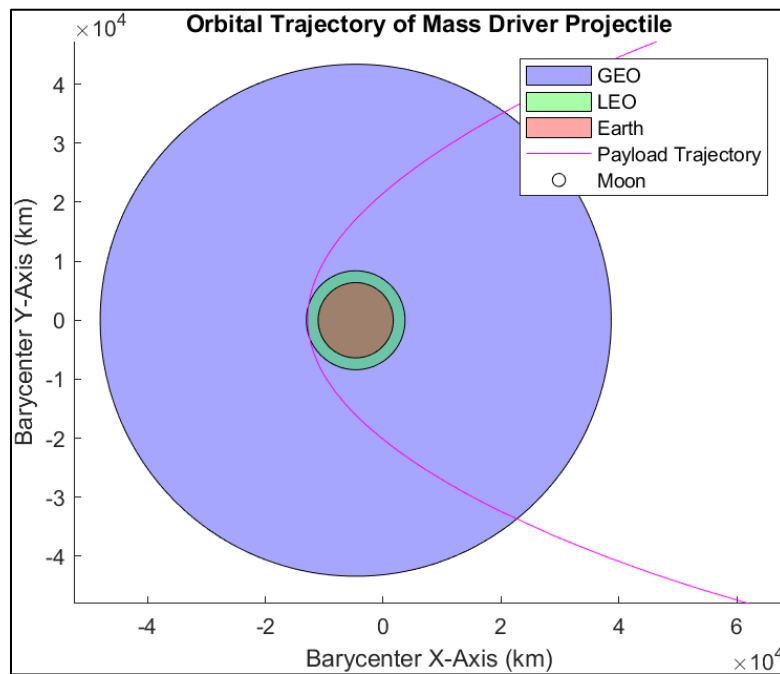## 7.5   Summary

Utilizing a circular planar restricted three-body approach, an orbital trajectory was identified which would result in a payload being launched from the lunar mass driver and eventually reaching LEO in approximately 2.14 days. The specific mass drive launch angle required to achieve this trajectory is 31°, so the lunar mass driver will be constructed on a line that is 31° from the Barycentric x-axis. An orbital platform or station in LEO will be required to collect the transported payload, but the design of such a station is beyond the scope of this project.

It is important to identify that several assumptions were made to simplify the three-body problem, making it more easily solvable. These assumptions include a circular orbit assumption, when the Moon does not orbit the Barycenter circularly, but rather it orbits elliptically. Additionally, the planar assumption assumes that the orbit lies on the ecliptic plane, when, since the payload is being launched from the lunar north pole, the orbit will not necessarily be planar. Finally, the restricted nature of the three-body problem ignores the mass of the payload and all other masses in the solar system. This assumption is largely valid, as the mass of the payload is mathematically insignificant compared to the masses of the Earth and the Moon, but the gravitational effects of the Sun are likely not as insignificant. Despite these assumptions, the results are acceptable, and should be within an acceptable margin of potential error.

8. External Considerations

8.1 Economic Considerations

The building of a lunar mass driver has some interesting economic ramifications. As mentioned in Section 1.1, the main resources transported by the mass driver are helium-3, ice, methane, and platinum. Of those, helium-3 and platinum are the two that would most likely be used on Earth.

Currently, helium-3 is primarily used for medical imaging and for nuclear fusion experiments. Due to the Earth's atmosphere protecting the Earth from solar wind, almost all helium-3 on Earth has been artificially created using an expensive process involving the radioactive decay of tritium, a hydrogen isotope primarily used in nuclear warheads. Introducing naturally occurring helium-3 from the Moon would likely dramatically reduce the price of helium-3. This would in turn likely reduce the cost of both medical imaging and nuclear fusion experiments.

Platinum is one of the rarer metals on Earth, consequently making it quite valuable. Unlike gold or silver, platinum has a limited number of potentially commercial or electronic applications. This has resulted in platinum being a symbol of wealth and status. The introduction of a new source of platinum might reduce the overall price of platinum, but since platinum has so few commercial applications, it is unlikely to have a major economic impact.

8.2 Environmental Considerations

A lunar mass driver itself has no major environmental considerations. However, a mass driver is predicated on the existence of a lunar mining operation that requires the existence of a reliable and cheap transportation system. A lunar mining operation does present some potential environmental considerations.

As discussed previously, the main materials transported back to Earth would be platinum and helium-3. However, both of those materials are relatively scarce on the Moon and would require something akin to strip mining to result in meaningful quantities of each material [1]. A mining operation on this scale would certainly do irrevocable harm to the lunar surface and environment. While there is no known ecosystem on the Moon to destroy, the geological state of the Moon would be forever altered, and the potential effects of strip mining the Moon are completely unknown.

8.3 Political Considerations

Problems with the construction of a lunar mass driver largely begin with political considerations. The Moon does not belong to any one country, and any attempt to build a structure on the Moon or to gather resources from the Moon's surface could result in major political backlash from foreign countries. Additionally, the building of a large mass driver could be seen as placing a potential weapon on the Moon, which would likely violate the 1967 Outer Space Treaty banning the militarization of celestial bodies [21].

Any successful effort to colonize, mine and transport resources from the Moon would require international cooperation through an organization such as the United Nations. Additional safeguards would have to be put in place to ensure the mass driver could not be easily weaponized by any one country or member state. It is also unlikely that the United Nations would allow private companies to mine the Moon, meaning that it would be up to international governments to build the lunar infrastructure necessary to operate a mass driver.

8.4   Ethical Considerations

The ethical considerations regarding the construction and operation of a lunar mass driver are largely related to considerations already outlined. There is a distinct ethical argument against mining the Moon and potentially destroying geological data pertaining to the early life of the Earth. Additionally, there is concern that a lunar mass driver could be weaponized, adding another potential weapon of mass destruction to the already sizeable international stockpile.

This particular design could not easily be weaponized as the acceleration and trajectory of the payload is determined by the size and angle of the mass driver. However, it is not impossible to transform the mass driver into a weapon capable of taking down satellites. Theoretically, by either reducing the charge within the capacitors or by changing the mass, the trajectory could be altered enough to turn the mass driver in a pseudo shotgun capable of damaging satellites in LEO and GEO. Safeguards during the actual implementation of the mass driver must be put in place to prevent the mass driver's weaponization.

8.5   Health Considerations

The mass driver is designed to be fully automated, making human technicians unnecessary. However, it is likely humans will be necessary to build this colossal structure. There are absolutely health risks to working in space, and the long-term effects of space are still being studied.

Since the mass driver is being positioned at the north pole to take advantage of nearly constant sun, anyone building the mass driver would be exposed to high amounts of solar radiation with minimal reprieve. Additionally, the Moon itself has no atmosphere so all construction would need to be done in spacesuits and any damage to the spacesuit could result in injury or death.

8.6   Manufacturing Considerations

Manufacturing the lunar mass driver is a major consideration. All of the individual components would need to be constructed on Earth and then sent into LEO before being transported to the Moon. The difficulty is combining all the components together on the lunar surface. Construction and manufacturing techniques have not been developed and tested in the vacuum of space, so new techniques would need to be created to enable the individual components to be connected.

The best method currently available would involve designing the mass driver into a series of identical modules which could be connected via a locking mechanism similar to the ones used during docking with the International Space Station (ISS). Breaking down the mass driver into a series of identical modules would also make manufacturing easier and faster and make testing each module easier. However, it also presents an issue that if there is a flaw in the module, there would be a flaw in all the modules.

9. Final Mass Driver System Design

9.1 Mass Driver Design Results

The mass driver shall transport at least 100,000 metric tons of lunar material each year back to LEO. This design accomplishes this goal by launching a 25.4 kg payload every 10 seconds. The mass driver consists of an accelerating section that is approximately 293 m in length which accelerates a payload bucket to a speed of 2.4 km/s, which is greater than the necessary 2.38 km/s required to escape the Moon's gravitational pull.

The decelerating section is approximately 202 m in length and will return the empty bucket back to the beginning of the accelerating section after slowing it down. The entire mass driver has an approximate mass of 424.8 metric tons and will be broken down into nearly identical modules which can be connected and assembled at the lunar north pole at an angle of 31° which will result in the proper trajectory. The mass driver will require 8.7 MW of power which will be generated using a field of solar panels. The overall system has a power efficiency of 84%.

9.2 Communications Subsystem Design Results

The communications subsystem for the mass driver provides a 25 kbps uplink and downlink between the mass driver and either an Earth ground station or a lunar colony ground station. This is accomplished using a dual-purpose 1.5 m diameter antenna with a diplexer enabling both uplink and downlink. The transmitter antenna gain is 37.2 dB while the receiver antenna gain is 37.7 dB. A binary phase shift keying system with RS Viterbi decoding will be used to minimize the BER and ensure effective and accurate data transfer.

9.3 Thermal Control Subsystem Design Results

The thermal control subsystem for the mass driver keeps the system below 400 K during operation and above 233 K during maintenance. This is accomplished by having a radiator area of approximately 6.2 m^2 for each 2 m long module, with the radiators using a Z93 white paint finish. Due to the mass driver being at the pole with almost constant sunlight, no active thermal system is necessary, however patch heaters will be added to each module in the event of a temperature emergency. The system will be monitored by a solid-state temperature controller linked to temperature sensors within each module. In the future, heat pipes can be added to the radiators to increase the efficiency of the radiators.

9.4 Electrical Power Subsystem Design Results

The electrical power subsystem for the mass driver will provide the necessary 8.7 MW of power over the course of a 20-year mission life cycle. This is accomplished using a massive 37,000 m^2 array of multijunction GaInP/GaInAs solar panels. The panels can either be attached to the superstructure of the mass driver, or can be placed elsewhere and the power can then be transferred to the mass driver.

An energy storage system consisting of stable lithium-ion batteries will be used to store power during eclipse and contains 2,240 W*hr. Specifically, it is a system with two batteries that are redundant where each battery has an energy capacity of 2,240 W*hr, which is enough to power the communications subsystem and the emergency patch heaters in eclipse if necessary. The energy storage system is not designed to power the entire mass driver during eclipse. Independent and unregulated chargers will be used for the batteries to improve battery life, and a DET will be used for power regulation.

9.5   Orbital Trajectory Results

The orbital trajectory for the mass driver payload was determined using a restricted circular planar three-body problem. Utilizing this three-body problem a sweep of mass driver launch angles was examined to find an angle resulting in a trajectory passing through LEO. The result was a single angle, 31°, which both passed through LEO and did not result in an impact with Earth. Utilizing this information, the mass driver will be built at a 31° angle from the axis drawn between the Earth and the Moon, about the axis of rotation of the Moon as shown in Figure 9.1.
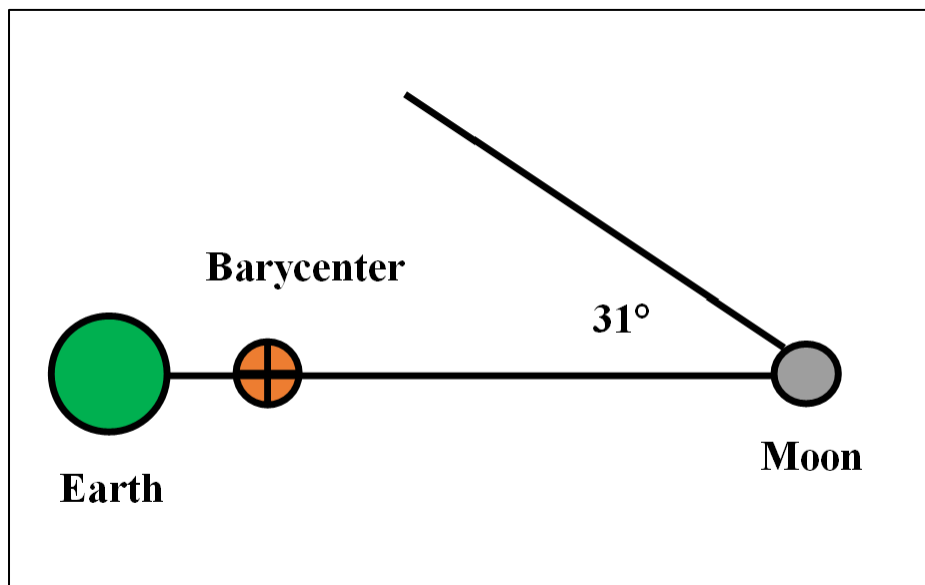

Figure 9.1- Mass driver angle from Earth-Barycenter-Moon axis

9.6   Design Conclusions

The mass driver design for this project was based largely on the work of Dr. O'Neill's team. With the preliminary work done by them, the details could be completed for this project. The result is a mass driver which transports 100,000 metric tons of lunar material from the lunar surface to LEO. The mass driver is designed to be broken down into 2-m long sections that are constructed on Earth, and then transported to the lunar north pole before being connected. The system is powered by a large array of solar panels and is capable of communication with both Earth and a lunar colony.

In the future, further work can be done narrowing down specific components and optimizing the internal workings of the mass driver, but that would require substantial physical construction and testing and is beyond the scope of the original definition of this project. This project focuses on the design of the subsystems supporting the mass driver and the determination of the orbital trajectory required to transfer the payload from the lunar surface to LEO, and the design outlined in this report accomplishes that task, meeting all of the requirements presented in the requirements section.

References

[1] Morton, O., *The Moon*, The Economist, London, England, June 2019, pp. 189-239.

[2] Aderin-Pocock, M., *The Book of the Moon: A Guide to Our Closest Neighbor*, Abrams Image, New York, April 2019, pp. 27-204.

[3] Stroud, R., *The Book of the Moon*, Walker Books, New York, June 2009, pp. 49-50.

[4] O'Neill, G. K., "Space Resources and Space Settlements," NASA SP-428, Summer 1977.

[5] Ernst, J., Lynds, R., Popescu, C., and Sutherland, M., "Ultra Capacitors – Capacitor Based Energy Storage," *International Exhibition and Conference for Power Electronics, Intelligent Motion, Renewable Energy and Energy Management*, PCIM, Nuremburg, Germany, 2017, pp. 622-7.

[6] Liles, K., and Amundsen, R. "NASA Passive Thermal Control Engineering Guidebook v3.1," NASA. April 2022.

[7] Stanley, S. M., and Luczaj, J. A., *Earth System History*, 4th ed., W. H. Freeman, New York, 2014, pp. 261.

[8] Galvez, R., Gaylor, S., Young, C., Patrick, N., Johnson, D., and Ruiz, J. "The Space Shuttle and Its Operations," NASA, retrieved March 1st, 2023.

[9] O'Neill, G. K., *The High Frontier*, 1st ed., Bantam Books, New York, 1977, pp. 134.

[10] Hanushek, E., "Testimony on Space Shuttle Pricing Policy," United States Senate, Washington, DC, March 1985, pp. 2.

[11] Robinson, K. F., Hefner, K., and Hitt, D., "NASA's Launch System – An Evolving Capability for Exploration," International Academy of Astronautics, Paper M15-4689, July 2015.

[12] "Falcon Payload User's Guide," SpaceX, September 2021.

[13] Meyer, C. "NASA Lunar Petrographic Educational Thin Set," NASA, 2003.

[14] Chu, P. P., and Kifle, M., "A Reconfigurable Communications System for Small Spacecraft," NASA E-14098, May 2004.

[15] Larson, W. J., and Wertz, J. R., "Spacecraft Subsystems," *Space Mission Analysis and Design*, 3rd ed., Microcosm Press, El Segundo, CA, 1999, pp. 353-518.

[16] Smitherman, D. V., "A Comparison of a Solar Power Satellite Concept to a Concentrating Solar Power System," AIAA 2013 Space Conference and Exposition, September 2013.

[17] Lyons, J., Fatemi, N., Gamica, R., Sharma, S., Senft, D., and Maybery, C., "Design and Development of the Space Technology 5 (ST5) Solar Arrays," 31st IEEE Photovoltaic Specialists Conference, January 2005.

[18] Takamoto, T., Sasaki, K., Agui, T., Juso, H., Yoshida, A., and Nakaido, K., "III-V Compound Solar Cells," *Sharp Technical Journal*, published 2010.

[19] Dalton, P. J., Schwanbeck, E., North, T., and Balcer, S., "International Space Station Lithium-Ion Battery," NASA Aerospace Battery Workshop, November 2016.

[20] Hunter, J. M., "Chapter 10: The Three-Body Problem," *AE 242 Orbital Mechanics and Mission Design: Astrodynamics Course Reader*, SJSU, San Jose, CA, 2022, pp. 126-136.

[21] "Treaties on Principles Governing the Activities of States in the Exploration and Use of Outer Space, including the Moon and other Celestial Bodies," United Nation Treaty 2222 (XXI), Dec. 1966.

Appendix A: Mass Driver Component Sizing Derivations

Bucket coil width:

$$W_B = 0.1 * D = (0.1)(0.637 \ m) = 0.0637 \ m \tag{A.1}$$

Effective radius of the bucket coil:

$$r = 0.26 * D = (0.26)(0.637 \ m) = 0.166 \ m \tag{A.2}$$

Length of single-turn drive winding:

$$\ell_w = \pi D = \pi(0.637 \ m) = 2.00 \ m \tag{A.3}$$

Inductance length or drive coil spacing:

$$\ell_m = 0.185 * D = (0.185)(0.637 \ m) = 0.118 \ m \tag{A.4}$$

Phase length of drive current oscillation:

$$\ell_p = 4 * \ell_m = 4 * 0.118 \ m = 0.472 \ m \tag{A.5}$$

Volume of individual bucket coils:

$$
\begin{aligned}
V_{BC} = \pi W_B &\left[\left(r + \frac{W_B}{2} \right)^2 - \left(r - \frac{W_B}{2} \right)^2 \right] \\
&= \pi(0.0637 \ m) \left[\left(0.166 \ m + \frac{0.0637 \ m}{2} \right)^2 \right. \\
&\left. - \left(0.166 \ m - \frac{0.0637 \ m}{2} \right)^2 \right] = 0.00318 \ m^3
\end{aligned}
\tag{A.6}
$$

Mass of a single bucket coil:

$$m_{BC} = V_{BC}\rho_s = (0.00318 \ m^3) \left(4530 \frac{kg}{m^3} \right) = 14.4 \ kg \tag{A.7}$$

Total coil mass per bucket:

$$m_{super} = 2 * m_{BC} = 2 * (14.4 \ kg) = 28.8 \ kg \tag{A.8}$$

Empty bucket mass:

$$m_B = 2 * m_{super} = 2 * (28.8 \ kg) = 56.6 \ kg \tag{A.9}$$

Loaded bucket mass:

$$m_{BL} = m_B + m_1 = 56.6 \ kg + 25.4 \ kg = 82 \ kg \tag{A.10}$$

Ratio of unloaded to loaded bucket mass:

$$m_B/m_{BL} = \frac{56.6 \ kg}{82 \ kg} = 0.69 \tag{A.11}$$

Current in each bucket coil:

$$i_B = 2.5 * 10^6 * D^2 = (2.5 * 10^6)(0.637 \ m)^2 = 1.01 * 10^6 \ A \tag{A.12}$$

Single-turn self-inductance of a drive coil:

$$H_S = (2.004 * 10^{-6}) * D = (2.004 * 10^{-6}) * (0.637 \ m) = 1.28 * 10^{-6} \ H \tag{A.13}$$

Total number of drive windings per phase:

$$N_W = 11.62 * v_e^2 * a^{-1} * m_1^{-\frac{1}{3}} = (11.62) \left(2400 \frac{m}{s}\right)^2 \left(9800 \frac{m}{s^2}\right)^{-1} (25.4 \ kg)^{-\frac{1}{3}} \tag{A.14}$$
$$= 2320$$

Appendix B: MATLAB Code

```matlab
%% Master's Project
%Ethan Miller
clc
clear
close all

%% Communications Analysis
%Constants
Link_m = 10; %Link Margin [dB]
Loss_i = -2; %Implementation Loss [dB]
BER = 10^-5; %Bit Error Rate
%Data_R = 25; %Data Rate [kbps]
Er = 0.2; %Receive Antenna Pointing Error [degrees]
Dr = 0.5:0.1:5; %Receive Antenna Diameter [m]
Se = 3.85*10^8; %Propogation Path Length to Earth [m]
Sm = 10000; %Propogation path Length to Lunar Base [m]
Et = 0.5; %Transmit Antenna Pointing Offset [degrees]
Dt = 0.5:0.1:5; %Transmit Antenna Diameter [m]
Ll = -1; %Transmitter Line Loss [dB]
f = 2; %Frequency [GHz]
L_ab = -3.4; %Absorption Loss [dB]
Ts = 135; %System Noise Temperature [K]
%EbNo_Req = 9.6;
EbNo_Req = [9.6 10.3 13.3 9.2 4.4 2.7 4.0]'; %EbNo Required for
QPSK and BER = 10^-5 [dB]
Eta = 0.55; %Antenna Smoothness Factor (1 is perfect)

%Calculating Data Rate
BitS = 5; %Number of bits per sample for 1.5% Accuracy
Sections = 248; %Total Number of 2m Sections/Modules
Data_time = 5; %Time between Data Bursts [s]
Samples = 1*Sections; %Number of Samples per data burst
Data_R = Samples/Data_time*BitS; %Data Rate [bps]

%Calculations
EbNo = EbNo_Req-Loss_i+Link_m; %Desired EbNo [dB]

%Calculating Carrier to Noise Density Ratio
CNo = EbNo + 10*log10(Data_R);

%Calculating Receive Antenna Gain
thetaR = 21./(f.*Dr); %Receiving Half-power Beamwidth [degrees]
Lpr = -12*(Er./thetaR).^2; %Receive Antenna Pointing Loss [dB]
Grp = 20*log10(pi)+20*log10(Dr)+20*log10(f*10^9)+10*log10(Eta)-
20*log10(3*10^8); %Peak Receive Antenna Gain [dB]
Gr = Grp+Lpr; %Receive Antenna Gain [dB]
```

```matlab
%Calculating Space Loss
Lse = 20*log10(3*10^8)-20*log10(4*pi)-20*log10(Se)-
20*log10(f*10^9); %Space Loss to Earth [dB]
Lsm = 20*log10(3*10^8)-20*log10(4*pi)-20*log10(Sm)-
20*log10(f*10^9); %Space Loss to Moon [dB]

%Calculating Transmit Antenna Gain
thetaT = 21./(f*Dt); %Transmitting Half-Power Beamwidth
[degrees]
Lpt = -12*(Et./thetaT).^2; %Transmit Antenna Pointing Loss [dB]
Gtp = 44.3-10*log10(thetaT.^2); %Peak Transmit Antenna Gain [dB]
Gt = Gtp+Lpt; %Transmit Antenna Gain [dB]

%Calculating EIRP
EIRPe = EbNo-Lse-L_ab-Gr-
228.6+10*log10(Ts)+10*log10(Data_R*100); %EIRP to Earth [dB]
EIRPm = EbNo-Lsm-L_ab-Gr-
228.6+10*log10(Ts)+10*log10(Data_R*100); %EIRP to Lunar Colony
[dB]
Pte1 = EIRPe-Ll-Gt; %Transmitter Power to Earth [dBW]
Ptm1 = EIRPm-Ll-Gt; %Transmitter Power to Lunar Colony [dBW]


%Calculating Transmitter Power
Pte2 = EbNo-Ll-Gt-Lse-L_ab-Gr-
228.6+10*log10(Ts)+10*log10(Data_R*100); %Transmitter Power to
Earth [dBW]
Ptm2 = EbNo-Ll-Gt-Lsm-L_ab-Gr-
228.6+10*log10(Ts)+10*log10(Data_R*100); %Transmitter Power to
Moon [dBW]
Pte = 10.^(Pte1/10); %Transmitter Power [W]
Ptm = 10.^(Ptm1/10); %Transmitter Power [W]

figure(1)
plot(Dt,Pte1(1,:),Dt,Ptm1(1,:))
xlabel('Transmitter Antenna Diameter (m)')
ylabel('Transmitter Required Power (dBW)')
title({'Effect of Transmitter Antenna Diameter on Required
Transmitter Power'})
legend('Mass Driver to Earth','Mass Driver to Lunar
Colony','location','NE')

figure(2)
plot(Dt,Pte1)
xlabel('Transmitter Antenna Diameter (m)')
ylabel('Transmitter Required Power (dBW)')
```

```matlab
title({'Effect of Transmitter Antenna Diameter on Required
Transmitter Power for','Mass Driver to Earth Ground Station
Transmission for','Various Modulation and Coding Schemes'})
legend('BPSK/QPSK','DPSK','FSK','8FSK','BPSK + R-1/2
Viterbi','BPSK + RS Viterbi','8FSK + R-1/2
Viterbi','location','NE')

%% Thermal Control System Analysis
%Constants
qsolarH = 1420*sind(0); %Solar Constant Hot Case [W/m^2]
qsolarC = 1360; %Solar Constant Cold Case [W/m^2]
MIR = 430; %Moon IR [W/m^2]
alphaH = 0.2; %Absorptance Hot Case
alphaC = 0.1; %Absorptance Cold Case
epsilonH = [0.72 0.78 0.85 0.88 0.92]'; %IR Emittance Hot Case
epsilonC = 0.78; %IR Emittance Cold Case
QintH = 5620; %Power Dissipation Hot Case [W]
%QintC = 0; %Power Dissipation Cold Case [W]
Boltz = 5.67*10^-8; %Boltzmann Constant [W/m^2K^4]
TradH = 380:2.5:500; %Max temperature [K]
TradC = 233; %Min Temperature [K]

%Radiator Sizing Hot Case
qExt = qsolarH+MIR;
A = QintH./(epsilonH.*Boltz.*TradH.^4-qExt);
QintC = Boltz*epsilonC*A*TradC^4-qExt*A;
Qrad = Boltz.*epsilonH.*A.*TradH.^4;
Qext = qExt*A;

figure(3)
plot(TradH,A)
xlabel('Maximum Temperature (K)')
ylabel('Radiator Area (m^2)')
title('Effect of Maximum Temperature and Reflective Coating on
Radiator Area')
legend('5 mil Aluminized Teflon (e = 0.72)','5 mil Silvered
Teflon (e = 0.78)','S13G-LO Paint (e = 0.85)','Chemglaze A276 (e
= 0.88)','Z93 Paint (e = 0.92)','location','NE')

figure(4)
plot(TradH,QintC)
xlabel('Maximum Temperature (K)')
ylabel('Heater Power during Cold Case (W)')
title({'Effect of Maximum Temperature and Reflective Coating
on','Heater Power during Cold Case'})
```

```matlab
legend('5 mil Aluminized Teflon (e = 0.72)','5 mil Silvered
Teflon (e = 0.78)','S13G-LO Paint (e = 0.85)','Chemglaze A276 (e
= 0.88)','Z93 Paint (e = 0.92)','location','SE')

%% Power System Analysis
Pe = 105; %Power in Eclipse [W]
Pd = 8.7*10^6; %Power in Daylight [W]
Te = 24*.2*3600; %Time in Eclipse [s]
Td = 24*.8*3600; %Time in Daylight [s]
Xec = 0.65; %Path efficiency in Eclipse
Xd = 0.85; %Path efficiency in Daylight
Cell = [0.208 0.218 0.199 0.257 0.280 0.358]'; %Cell Efficiency
Id = 0.77; %Inherent Degredation
ThetaI = 0:1:45; %Sun Incidence Angle [degrees]
Table = [10 33 155 33 15 12]'; %Years for 15% degradation [year]
Deg = 1-0.85.^(1./Table); %Degredation per Year [%/year]
Life = 20; %Mission Life [Year]

Psa = (Pe*Te/Xec+Pd*Td/Xd)/Td; %Power of Solar Array
P0 = 1367*Cell; %Power Output of Cell [W/m^2]
Ld = (1-Deg).^Life; %Lifetime Degredation
P_BOL = P0.*Id.*cosd(ThetaI); %Power at Beginning of Life
[W/m^2]
P_EOL = P_BOL.*Ld; %Power at End of Life [W/m^2]
A_sa = Psa./P_EOL; %Solar Array Area [m^2]

figure(5)
plot(ThetaI,A_sa)
title('Effect of Sun Incidence Angle on Solar Array Area')
xlabel('Inidence Angle [degrees]')
ylabel('Solar Array Area [m^2]')
legend('Silicon','Gallium Aresenide','Indium
Phosphide','Multijunction GaAs','Emcore ATJ','Multijunction
GaInP/GaAs/GaInAs','location','NW')

%Theoretical Efficiencies
CellT = 0.1:0.01:0.5;
ThetaIT = 15;
TableT = [10 12 16 22 30 40]';
DegT = 1-0.85.^(1./TableT);
P0T = 1367*CellT;
LdT = (1-DegT).^Life;
P_BOLT = P0T.*Id.*cosd(ThetaIT);
P_EOLT = P_BOLT.*LdT;
A_saT = Psa./P_EOLT;

figure(6)
```

```matlab
plot(CellT,A_saT)
title({'Effect of Solar Panel Efficiency on Solar Array Area at
Incidence','Angle = 15 degrees'})
xlabel('Solar Panel Efficiency')
ylabel('Solar Array Area [m^2]')
legend('Degradation = 1.61%/year','Degradation =
1.35%/year','Degradation = 1.01%/year','Degradation =
0.74%/year','Degradation = 0.54%/year','Degradation =
0.41%/year','location','NE')

%Energy Storage Calculations
Cycle = 20*365+5; %Number of discharge cycles
DOD = 0.25; %Depth of Discharge
Nbatt = 1; %Number of batteries making up Storage System
ncharge = 0.9; %Charging efficiency

Cb = Pe*Te/DOD/Nbatt/ncharge/3600; %Required Battery Capacity

%% Orbital Analysis
%Restricted Planar Circular Three Body Problem [Earth-Moon-Rock]
%Constants
Me = 5.9722e24; %Mass of Earth [kg]
Mm = 7.3477e22; %Mass of Moon [kg]
G = 6.6743e-20; %Gravitional Constant [N*km^2/kg^2]
Re = 6378; %Mean Radius of Earth [km]
Rm = 1737.4; %Mean Radius of Moon [km]
Rem = 384400; %Mean Distance between Earth and Moon [km]
Tau = 2*pi*Rem^1.5/sqrt(G*(Me+Mm)); %Orbital Period [s]
tf = 300000; %Final time [s]
V0 = -2.4; %Mass Driver Exit Velocity [km/s]
Theta = 22; %Angle of Mass Driver relative to Barycenter X-Axis
[degrees]

%Defining the Barycenter
Xe = -Rem*Mm/(Mm+Me); %Distance from Earth to Barycenter [km]
Xm = Rem*Me/(Mm+Me); %Distance from Moon to Barycenter [km]
W = 2*pi/Tau; %Angular Velocity of Barycenter in Newtonian Sun
Frame [rad/s]

%Defining Initial Conditions
x0 = Xm; %Initial Distance from Barycenter in X-Direction [km]
xdot0 = V0*cosd(Theta); %Initial Velocity in X-Direction [km/s]
y0 = 0; %Initial Distance from Barycenter in Y-Direction [km]
ydot0 = V0*sind(Theta); %Initial Velocity in Y-Direction [km/s]

%Equations of Motion for Rock using Barycenter Coordinates
```

```
%xddot-2*W*ydot+(G*(Me/Re^3+Mm/Rm^3)-W^2)*x =
G*Mm*Me*Rem/(Rm^3*(Me+Mm))-G*Me*Mm*Rem/(Re^3*(Me+Mm));
%Barycenter X Direction
%yddot+2*W*xdot+(G*Me/Re^3+G*Mm/Rm^3-W^2)*y = 0; %Barycenter Y
Direction
%zddot+(G*Me/Re^3+G*Mm/Rm^3)*z = 0; %Barycentric Z Direction

%Setting up ode45
tspan = [0 tf]; %Time span used by ode45
IC = [x0 xdot0 y0 ydot0]; %Initial Conditions [km km/s]
[t, x] = ode45(@fun, tspan, IC);
X = x(:,1);
Xdot = x(:,2);
Y = x(:,3);
Ydot = x(:,4);

%Generating a Circle for Earth
Earth = nsidedpoly(1000, 'Center', [Xe 0], 'Radius', Re);

%Generating a Circle for LEO
LEO = nsidedpoly(1000, 'Center', [Xe 0], 'Radius', Re+2000);

%Generating a Circle for GEO
GEO = nsidedpoly(1000, 'Center', [Xe 0], 'Radius', Re+37000);

%Plotting the position of Mass Driver Rock
hold on
figure(7)
plot(GEO, 'FaceColor', 'b')
plot(LEO, 'FaceColor', 'g')
plot(Earth, 'FaceColor', 'r')
plot(X,Y,'-m',Xm,0,'ok')
title('Orbital Trajectory of Mass Driver Projectile')
xlabel('Barycenter X-Axis (km)')
ylabel('Barycenter Y-Axis (km)')
legend('GEO','LEO','Earth','Payload Trajectory','Moon')
axis equal

%Determine time required to reach GEO
tGEO = find(X < Re+37000+Xe & Y < Re+37000 & X > -(Re+37000)+Xe
& Y > -(Re+37000));
timeGEO = tGEO(1)/length(t)*tf/3600/24

%Determine time required to reach LEO
tLEO = find(X < Re+2000+Xe & Y < Re+2000 & X > -(Re+2000)+Xe & Y
> -(Re+2000)); %Dummy Variable finding LEO time
```

```matlab
timeLEO = tLEO(1)/length(t)*tf/3600/24 %Time to reach LEO in
days

%Determine if payload impacts Earth
tEarth = find(X < Re+Xe & Y < Re & X > -Re+Xe & Y > -Re);
timeEarth = tEarth(1)/length(t)*tf/3600/24

function dRdt = fun(t,x)
        X = x(1);
        Xdot = x(2);
        Y = x(3);
        Ydot = x(4);
        Me = 5.9722e24; %Mass of Earth [kg]
        Mm = 7.3477e22; %Mass of Moon [kg]
        G = 6.6743e-20; %Gravitional Constant [N*km^2/kg^2]
        Rem = 384400; %Mean Distance between Earth and Moon [km]
        W = sqrt(G*(Me+Mm)/Rem^3); %Angular Velocity of
Barycenter in Newtonian Sun Frame [rad/s]
        Xe = Rem*Mm/(Mm+Me); %Distance from Earth to Barycenter
[km]
        Xm = Rem*Me/(Mm+Me); %Distance from Moon to Barycenter
[km]
        Pi1 = Me/(Me+Mm); %Dummy Variable
        Pi2 = Mm/(Me+Mm); %Dummy variable
        dRdt = [Xdot;2*W*Ydot+W^2*X-
G*Me/(sqrt((X+Xe)^2+Y^2))^3*(X+Pi2*Rem)-
G*Mm/(sqrt((X+Xm)^2+Y^2))^3*(X-Pi1*Rem);Ydot;-2*W*Xdot+W^2*Y-
(G*Me/(sqrt((X+Xe)^2+Y^2))^3-G*Mm/(sqrt((X+Xm)^2+Y^2))^3)*Y];
end
```